OPEN ACCESS Freely available online

AFM Applied Functional Materials

ISSN 2737-5323
Volume 2, Issue 1
https://www.iikii.com.sg/journal/AFM
Applied Functional Materials

Article

Failure Behaviour of Carbon-Epoxy Composite in Crack Arrester and Crack Divider Mode

Majee Kumar Swarup [1,*], Das Jiten [2], S Seetaraman [1]

[1] Advanced Systems Laboratory, Hyderabad, India; swarup_majee@yahoo.co.in, swarupkumarmajee123@gmail.com
[2] Defence Metallurgical Research Laboratory, Hyderabad, India; dasjiten@rediffmail.com
* Correspondence: swarup_majee@yahoo.co.in

Received: Feb 3, 2022; **Accepted:** Mar 3, 2022; **Published:** Mar 30, 2022

Abstract: Failure behaviour of a carbon-epoxy composite is studied both in crack arrester (CA) and crack divider(CD) mode by conducting 3-point bend test of un-notched (UN) and single edge pre-crack notched (N) (notch depth varied from 0.5 to 3.3 mm) specimens at various cross head speeds(CHS) such as 0.2, 50, 100, 200 and 500 mm/min. Influence of notch depth (ND) and CHS on the conditional fracture toughness(CFT) is understood using ANOVA. In both the mode, while the CFT values varies linearly with CHS, its values are observed to be lower at short ND, higher at medium ND and again lower at high ND. In both the modes at high ND (~3.3mm) opening mode/fibre breaking (mode I) failure occurs because of high crack tip stress concentration (as analysed from ANSYS 15.0) which cause fibre failure at the tip and corresponding Mode I fracture toughness was observed to be~20 MPa.m0.5. The composite also shows similar flexural strength both in CA mode (641+48) and in CD mode (634+49 MPa). In CD mode N specimen predominantly fails by mode I. While in CD mode the delamination (mode II) is only observed in UN specimens, in CA mode UN or small N specimen shows mode II failure and medium notched specimen shows mixed mode failure. In CA mode, number of delaminated layer is higher for the specimen tested at high CHS. In CA mode during charpy test (strain rate 103/s), the composite shows numerous delamination and absorbed much higher energy(~40J/cm^2) than that in CD (~10J/cm^2) mode where mode I failure is predominant. During impact test, lowering of test temperature to -40^{o}C has very little effect on the impact energy since it does not significantly affect the mode of failure.

Keywords: Crack arrester mode, Crack divider mode, Fracture toughness, Carbon-epoxy composite

1. Introduction

Carbon epoxy composite finds extensive application in defence, aerospace and automobile industries because of its very low density combined with very high modulus, strength, fatigue and corrosion resistance [1,2]. Ricardo Baptista et al. [3] found that the modulus and strength of the composite could be further improved by the elimination of the porosity in the epoxy matrix by graphite filler. Interfacial bonding between carbon fibre and the epoxy matrix is studied in great extent by the several researchers. They claimed to have improved interfacial bonding by incorporating graphene oxide [4] and carbon nanotubes (CNTs) [5]. J M F de Paiva et al. observed that plain weave fibre fabric shows better 'interlaminar shear properties' than that of eight harness satin [6]. Bouette et al. examined the influence of loading rates on the 'interlamellar shear strength' and shear modulus of the composite [7]. The researchers also carried out extensive study on the factors influencing the growth of delamination under different kind of loading [8]. Although delamination (mode II failure) may be the major cause of failure in crack arrester mode of testing, fibre breaking (mode I) may be the major cause of failure in crack divider mode. In the actual application, especially in space and defence applications, both kind of loading is present. As for example in cylindrical pressure vessel, as shown schematically in Fig. 1, both hoop stress (or circumferential stress) and longitudinal stress are present. If the carbon fibre fabrics are oriented circumferentially and stacked radially as shown in Fig. 1, the effect of hoop stress on failure beviour can be evaluated by three point bend testing in crack arrester mode. On the other hand, effect of longitudinal stress on the failure behaviour can be evaluated by three point bend test in crack divider mode.

Although several literatures describe the failure behaviour by delamination (mode II) which is mainly observed in the samples tested in crack arrester mode, failure behaviour of the composite in crack divider mode is scanty. However, there is significantly different failure mechanism (mode I/mode II/mixed mode) exists in these two different modes of testing. Furthermore, some researchers claimed to have found significant influence of strain rate on failure mechanism [9-12], while others found its weak influence failure mechanism and consequently on the mechanical behaviour of the composite [13]. On the other side, Lenda and

Mridha's work clearly shows that the impact strength of carbon epoxy composite significantly decreases when tested at subzero temperature [14]. This phenomena significantly hamper composites usefulness at subzero temperature. As the carbon epoxy composite is extensively used in defence and civilian application (as for example Boeing solely uses almost 50% ceramic fibre reinforced polymer composites), this composite is vulnerable to be hit by projectiles, and other flying objects. Therefore, several literature describes the effect of loading rate on the fracture toughness of the composite [15-20].

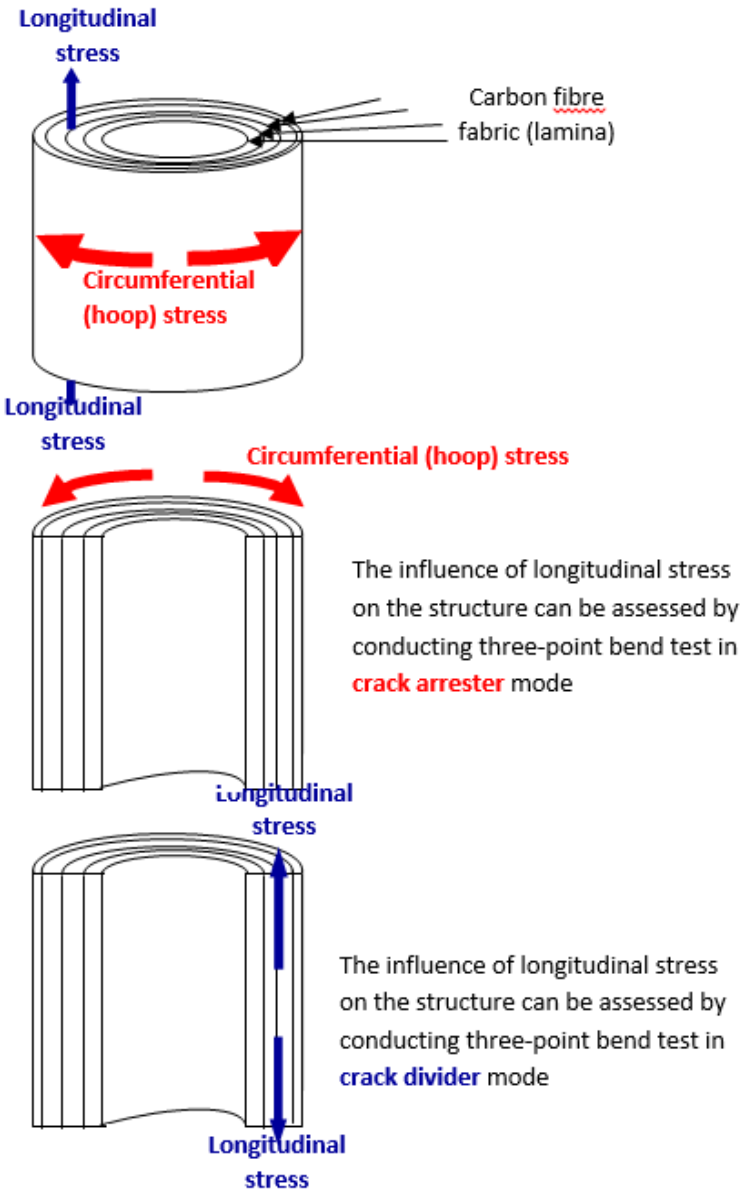

Fig. 1: Schematic of the presence of both hoop stress (or circumferential stress) and longitudinal stress in a hollow cylindrical vessel.

Although numerous author describe the influence of discontinuity/porosity, strain rate, temperature on the mechanical properties the carbon-epoxy composite, the effect of these parameters on the fracture/failure behaviour (i.e. mode I/mode II/mixed mode) of the composite is scanty. In order to understand the effect of porosity/discontinuity, and strain rate on the mechanical properties of the composite in both crack arrester and crack divider mode, a systematic failure investigation study (i.e. mode I/mode II/mixed mode) is carried out after conducting three-point bend test of single edge pre-crack notch and un-notched specimens. While the pre-crack notch depth was varied from 0.5-7 mm, specimen thickness was varied from 8mm to 10 mm. Samples were tested at crack divider orientation as well as crack arrester orientation with various cross head speeds such as 0.2, 50, 100, 200 and 500 mm/min. At the end, charpy impact test (strain rate 10^3/s) of a few single edge pre-crack notch and un- notched specimens for both crack arrester and crack divider orientation is also carried out for both room and subzero temperature (-40^{o}C) in order to understand the effect of temperature and notch depth and loading rate on failure mode (i.e. mode I/mode II/mixed mode) and consequently on

the impact energy absorption by the composite. Here, some effort has already been made to correlate the mode of failure (i.e. mode I/mode II/mixed mode) with the absorption of impact energy by the composite.

2. Experimental Methods

Carbon fibre (46-64 volume%) reinforced epoxy (34-42 volume%) composite was prepared from pre-impregnated fabrics (or pre-preg) which were prepared by dipping carbon fibre fabric in epoxy resin. These pre-pregs (as shown in Fig. 2) are cut into desired shape and sizes and stacked with an alternate pre-preg layers of 0 and 90^{o} orientation to get desired thickness. The stacked pre-pregs are then pressed and kept in vacuum and cured at the required temperatures to obtain composite with desired dimensions. Several samples (59 Nos.) as shown in Fig. 3 with dimension 6mm X 8mm X 90mm were extracted for testing in crack arrester and crack divider mode by three-point bend test using Instron 8800 at different cross head speeds (for eg.0.2, 50, 100, and 500 mm/min). In the samples which are to be tested in crack arrester mode, horizontally placed carbon fibre fabrics are stacked vertically. On the other hand, in the samples which are to be tested in crack divider mode, vertical carbon fibre fabrics are stacked horizontally as shown in Fig. 3. The schematic of the orientation of carbon fibre fabric lamina with respect to loading direction in both crack arrester and crack divider mode are shown in Fig. 4. Samples were made without (as schematically shown in Fig. 4) or with different depth of single edge notch (as schematically shown in Fig. 5). Samples without or with single edge notch of various depth (0.5-3.0mm) were three-point bend tested in both crack arrester and crack divider mode using Instron 8800 at different cross head speeds (for eg.0.2, 50, 100, and 500 mm/min). A few samples with higher thickness (10mm) and larger notch depth (7mm) were also three point bend tested in both crack arrester and crack divider mode to ensure opening mode (mode-I) failure for determining mode-I fracture toughness (K1c) of the composite.

Fig. 2: Image of carbon fibre pre-impregnated fabrics fabric or pre-preg used in this study for preparation of the composite.

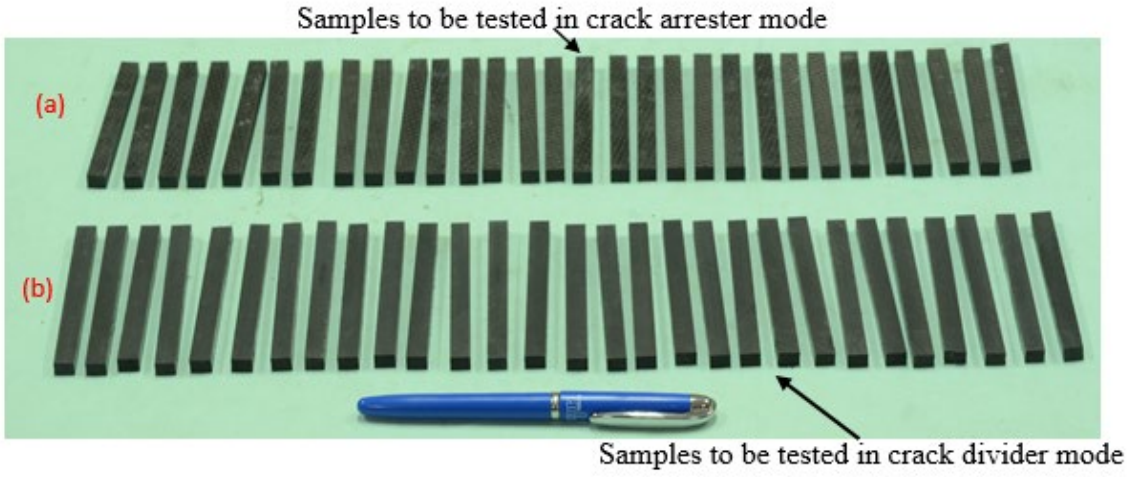

Fig. 3: Photographs of the extracted composite samples (6mm thicknessX8mm breadthX90mm length) (before making single edge notch) which are to be tested in crack arrester (a) and crack divider mode (b) respectively.

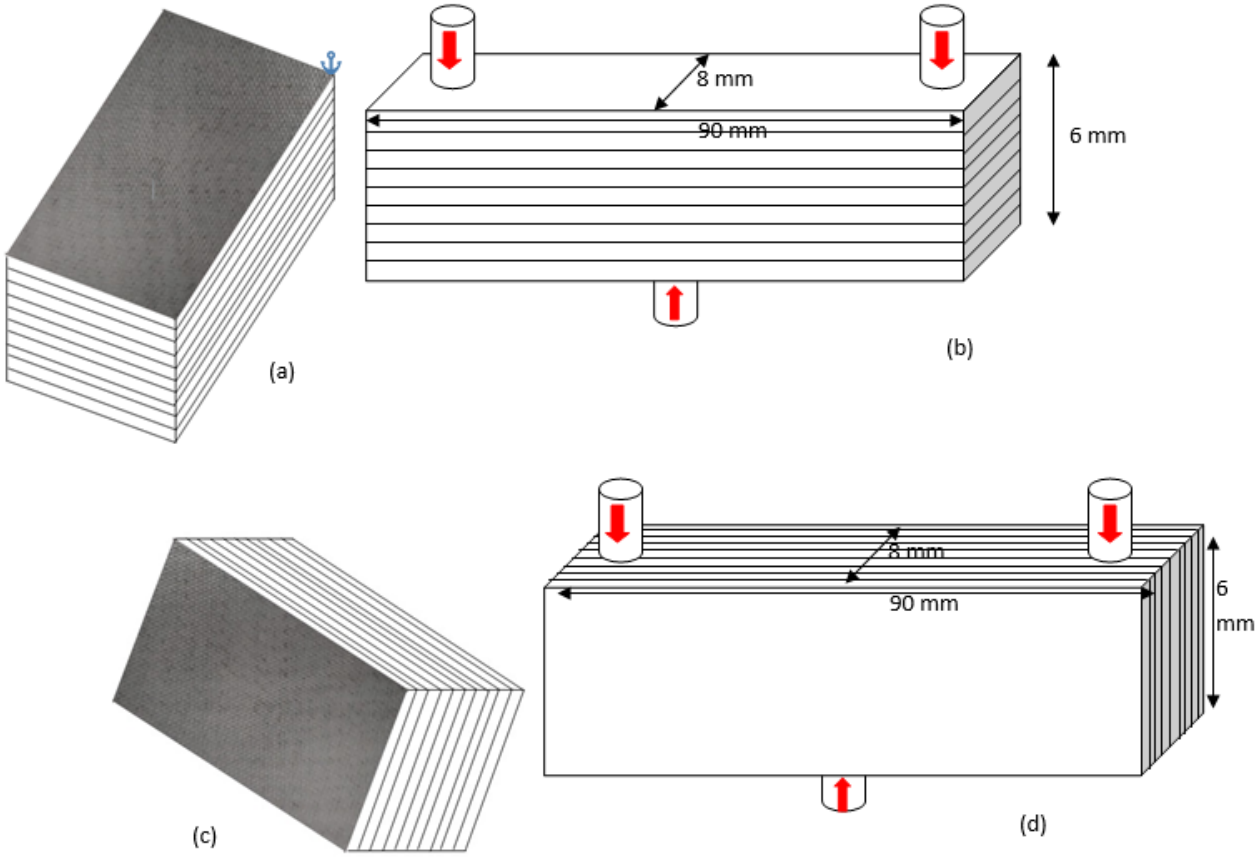

Fig. 4: Schematic of orientation of carbon fibre fabric (a and c) and loading direction (b and d) for the composite to be tested in crack arrester and crack divider mode respectively.

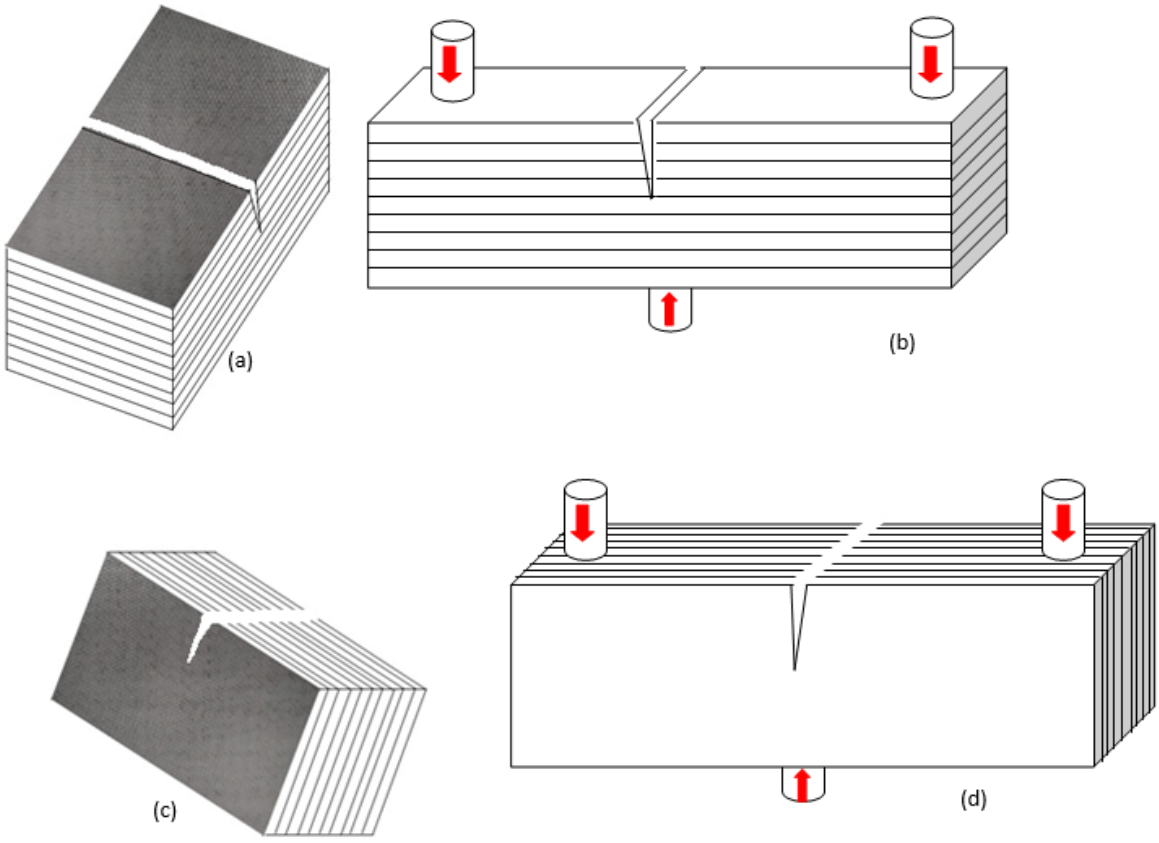

Fig. 5: orientation of single edge notch and carbon fibre fabric (a and c) as well as loading direction(b and d) for the composite to be tested in crack arrester and crack divider mode respectively.

Microstructural investigation of the sample before and after the three-point bend test were undertaken using optical and scanning electron microscope. A typical optical image of a sample with 0.5mm deep single edge notch which is to be tested in crack divider mode is shown in **Fig. 6** and orientation of the carbon fibre fabric is clearly shown in **Fig. 7**. Failed sample after three-point bend test both in crack arrester and crack divider mode are observed under scanning electron microscope in order to assess the crack origin and mode of failure.

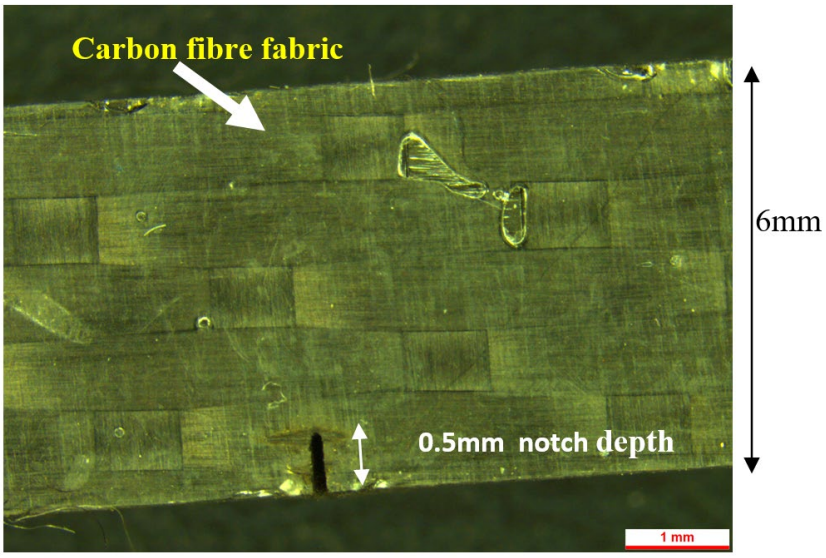

Fig. 6: Typical optical image of One sample with 0.5mm deep single edge notch to be tested in crack divider mode.

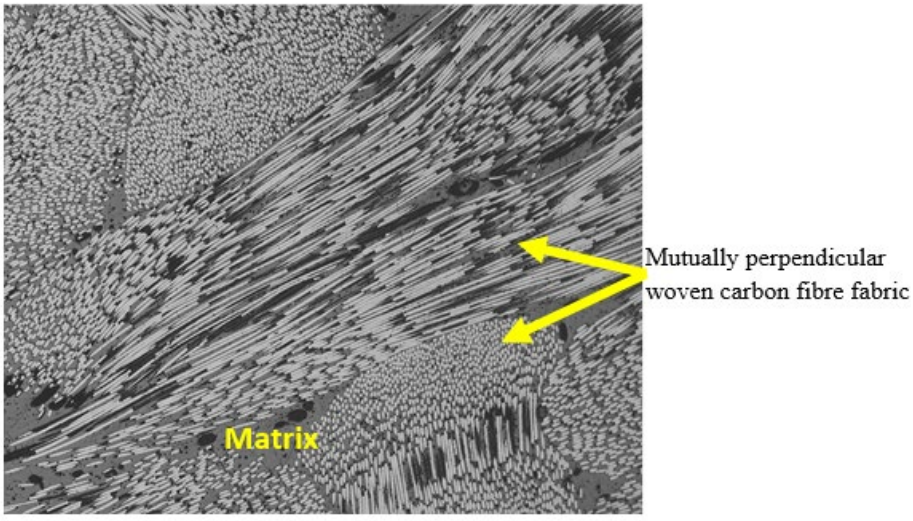

Fig. 7: Typical optical image of carbon fibre fabric and epoxy matrix in carbon-fibre epoxy composite.

Finally Charpy impact test of single edge pre-crack notch and un-notched specimens for both crack arrester and crack divider orientation is also carried out for both room and subzero temaperature (-40°C) at a strain rate of 10^3/s. The charpy test was carried out using charpy impact testing machine (Make: Fuel Instrument and Engineers Pvt. Ltd.).

3. Results

3.1. Three point Bend Test

The composite shows similar flexural strength both in crack arrester mode (641±48) and in crack divider mode (634±49 MPa). It is observed from **Fig. 8** that three-point bend test in crack arrester mode causes delamination in notched and unnotched samples. However, the samples which have single edge notch depth more than or equal to 2.5mm failed predominantly by carbon fibre breaking instead of delamination. Load vs. Displacement curve shows that stiffness of the sample decreases with the depth of single edge notch. Load vs. Displacement curves are characterized by sharp rise of load value followed by sharp drops and again followed by few spikes and drops of load value with displacement. However, the sharpness in rise and fall of load values decreases with the increase of the depth of notch.

Fig. 9 shows that three-point bend test in crack divider mode causes delamination in unnotched samples. However, the notched samples failed predominantly by carbon fibre breaking in stead of delamination. Load vs. Displacement curve shows that maximum load values are lesser for similar samples which are tested in crack divider mode than those tested in crack arrester mode (refer Fig. 10 and Fig. 11). Although stiffness of the unnotched samples tested in crack divider mode are less than those tested in crack arrester mode, the stiffness remain unaffected with the depth of notch, unlike the samples tested in crack arrester mode. Load vs. Displacement curves in crack divider mode are characterized by gradual rise of load value followed by gradual drops of load value with displacement. However, no rise and fall of load values are observed subsequently. It is important to note here that in case of crack arrester mode, initial peaks (i.e. maximum peaks or peak loads, Fig. 10) are sharper at shorter notch depth and gradually becomes broader with the increase of notch depth. However, in case of crack divider mode, breadths of these initial peaks (Fig. 11) remain independent of the notch depth. Although the initial peaks (i.e. maximum peak or peak load) in case of unnotched/short notched samples tested in crack arrester mode are much sharper that those tested in crack divider mode, the breadth of the initial peaks becomes similar for both the modes for the larger notch depth.

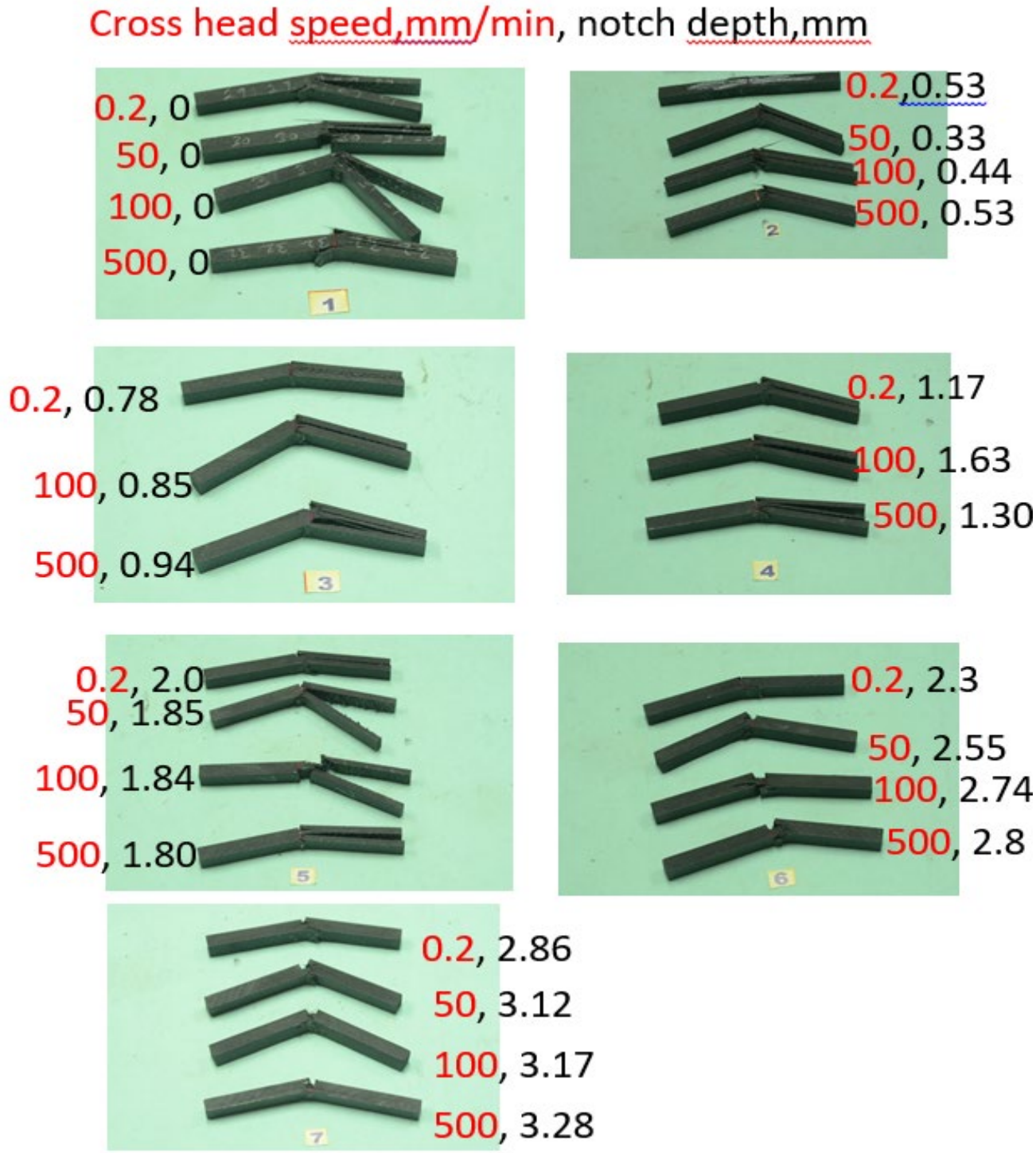

Fig. 8: Photographs of the three point ben9d tested samples in crack arrester mode at the respective cross head speed and notched depth mentioned against the photograph.

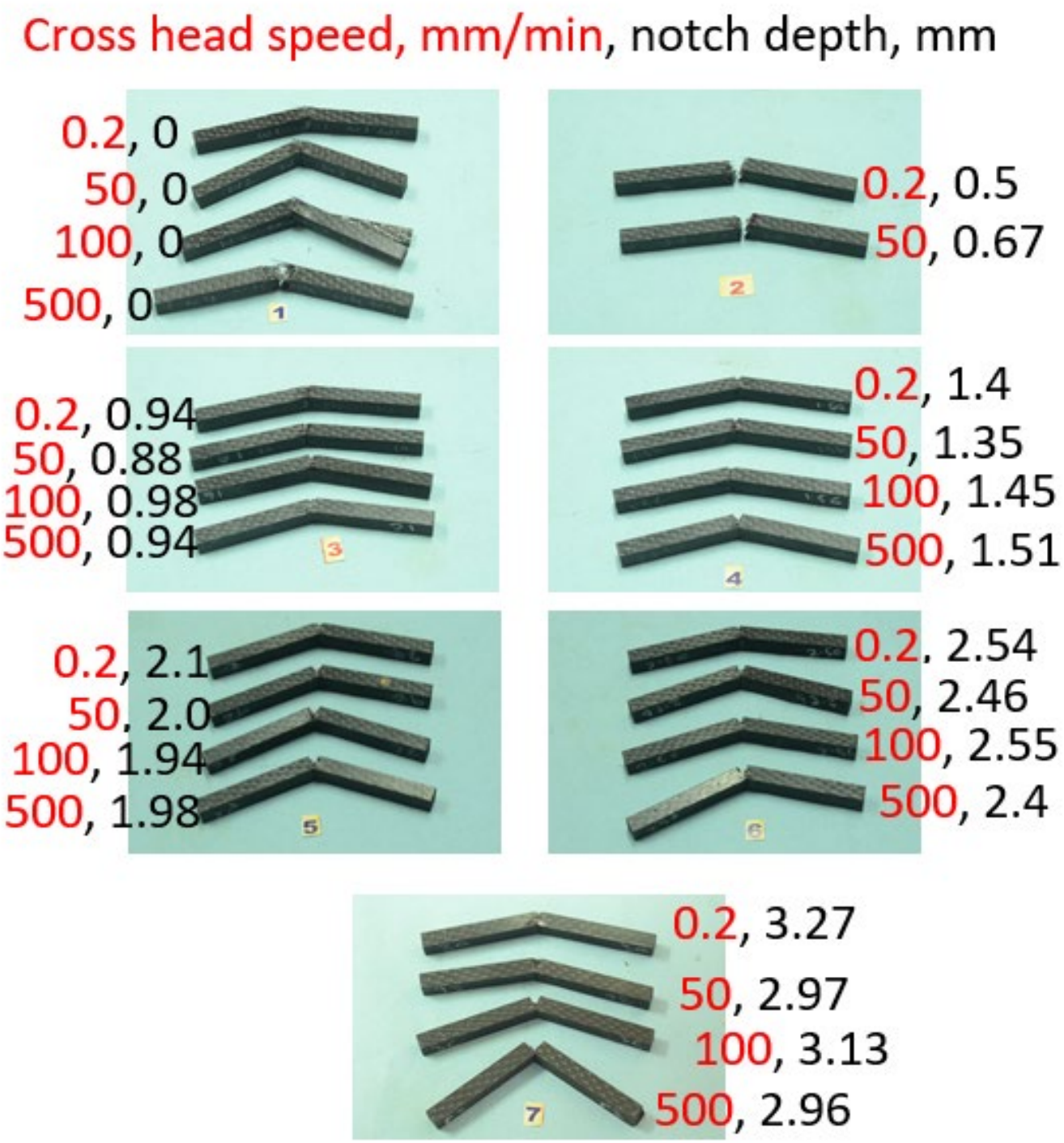

Fig. 9: Photographs of the three point bend t1e0sted samples in crack divider mode at the respective cross head speed and notched depth mentioned against the photograph.

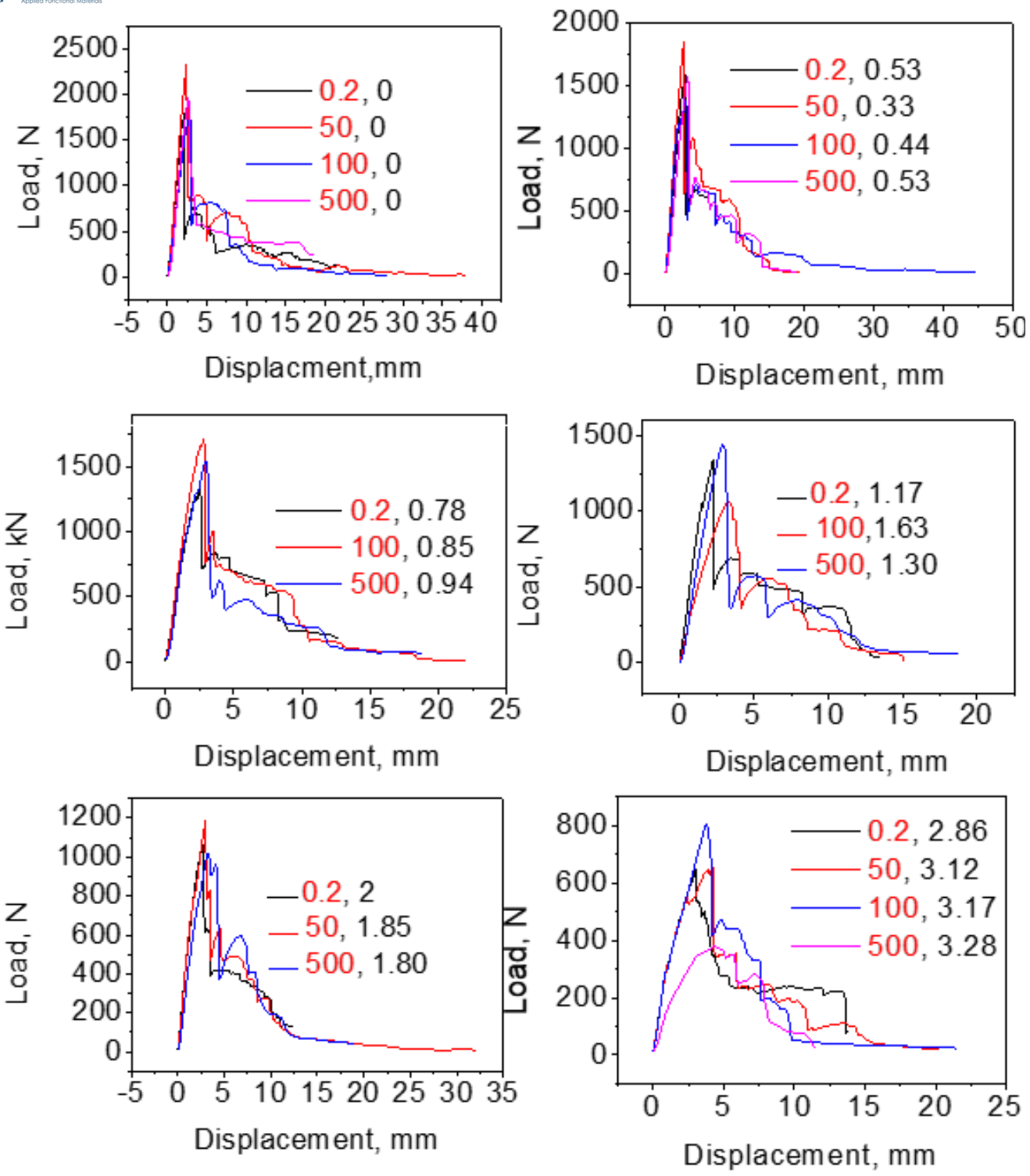

Fig. 10: Load vs. Displacement curves for three point bend tested samples in crack arrester mode. The respective cross head speed and notch depth are mentioned against the curves.

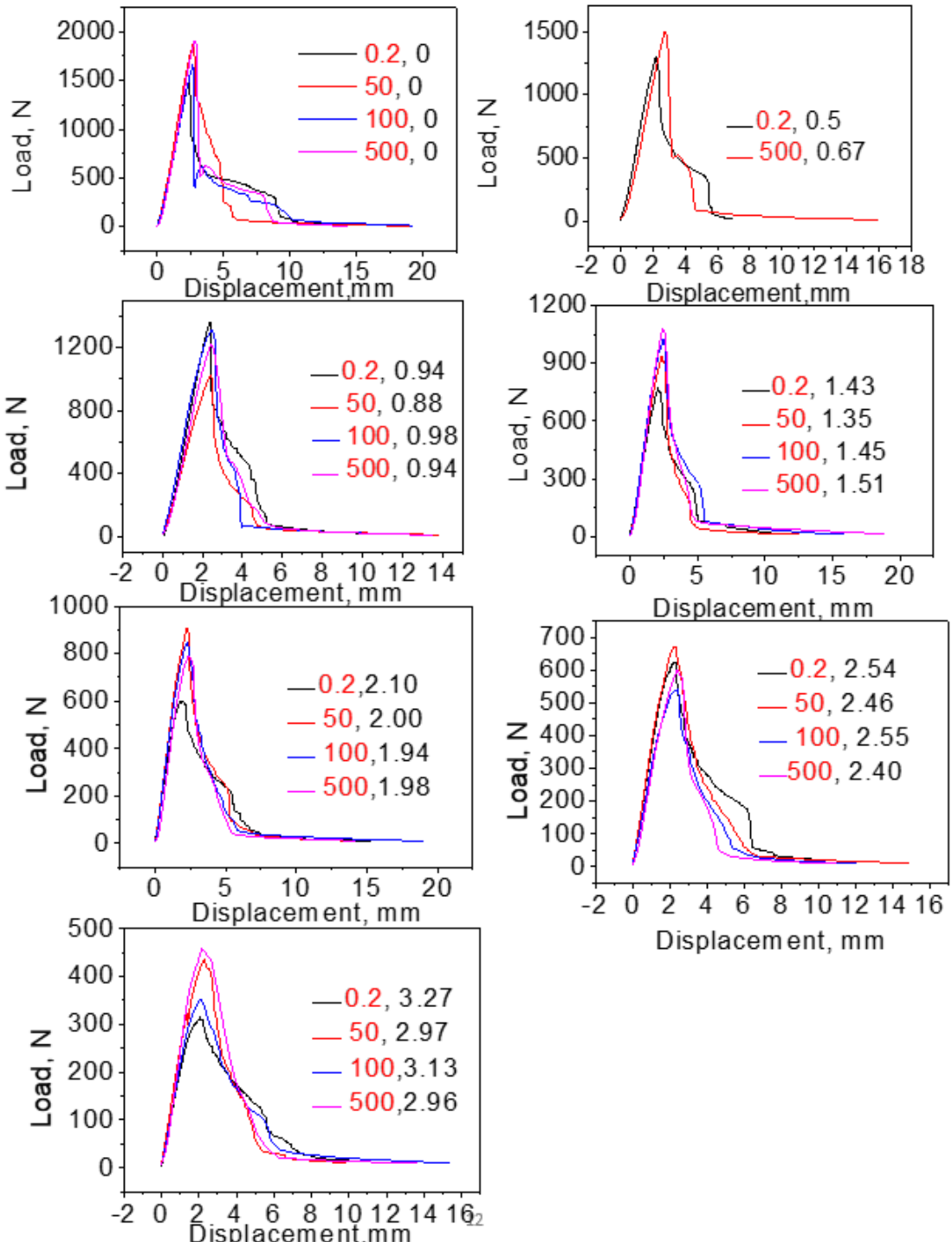

Fig. 11: Load vs. Displacement curves for three point bend tested samples in crack divider mode. The respective cross head speed and notch depth are mentioned against the curves.

The conditional fracture toughness as a function of notch depth irrespective of cross head speed is shown in Fig. 12 for both crack arrester and crack divider mode. The fracture toughness for the samples tested in crack arrester mode is found to be slightly higher than those tested in crack divider mode irrespective of the notch depth of cross head speed. Variation of coditional fracture toughness with cross head speed and notch depth is shown in Table 1. The correlation of the conditional fracture toughness with both cross head speed (or strain rate) and notch depth established using ANOVA in Minitab software for both crack arrester and crack divider mode. The analysis results are shown in Fig.s 13 and 14 for both crack arrester and crack divider respectively. From this analysis it is observed that the higher the cross head speed, the higher is the conditional fracture toughness for both the mode. It is also observed that for both the mode conditional fracture toughness is lower at very short and long notch depth and it is higher at intermediate notch depth.

Table 1: Variation of coditional fracture toughness with cross head speed and notch depth

Crack arrester mode				Crack divider mode		
Cross head speed	Pre-crack notch depth	Conditional fracture toughness		Cross head speed	Pre-crack notch depth	Conditional fracture toughness
0.2	0.53	23.26412		0.2	0.5	18.35924
50	0.33	20.9401		500	0.67	25.99957
100	0.44	19.23644		0.2	0.94	26.82811
500	0.53	22.53792		50	0.88	20.59369
0.2	0.78	22.26787		100	0.98	25.43705
100	0.85	27.35692		500	0.94	23.76667
500	0.94	25.61941		0.2	1.43	20.25719
0.2	1.17	25.57349		50	1.35	22.4324
100	1.63	26.15925		100	1.45	25.50869
500	1.3	31.72238		500	1.51	25.99166
0.2	2	26.61046		0.2	2.1	19.7665
50	1.85	30.43255		50	2	28.81572
100	1.84	26.04322		100	1.94	23.89714
500	1.8	26.46533		500	1.98	23.81605
0.2	2.3	22.60262		0.2	2.54	23.98741
50	2.55	26.03662		50	2.46	25.40036
100	2.74	30.91878		100	2.55	22.00545
500	2.8	24.97174		500	2.4	22.73472
0.2	2.86	22.97712		0.2	3.27	18.05193
50	3.12	25.6384		50	2.97	20.37149
100	3.17	34.41363		100	3.13	19.58874
500	3.28	20.42291		500	2.96	20.92382

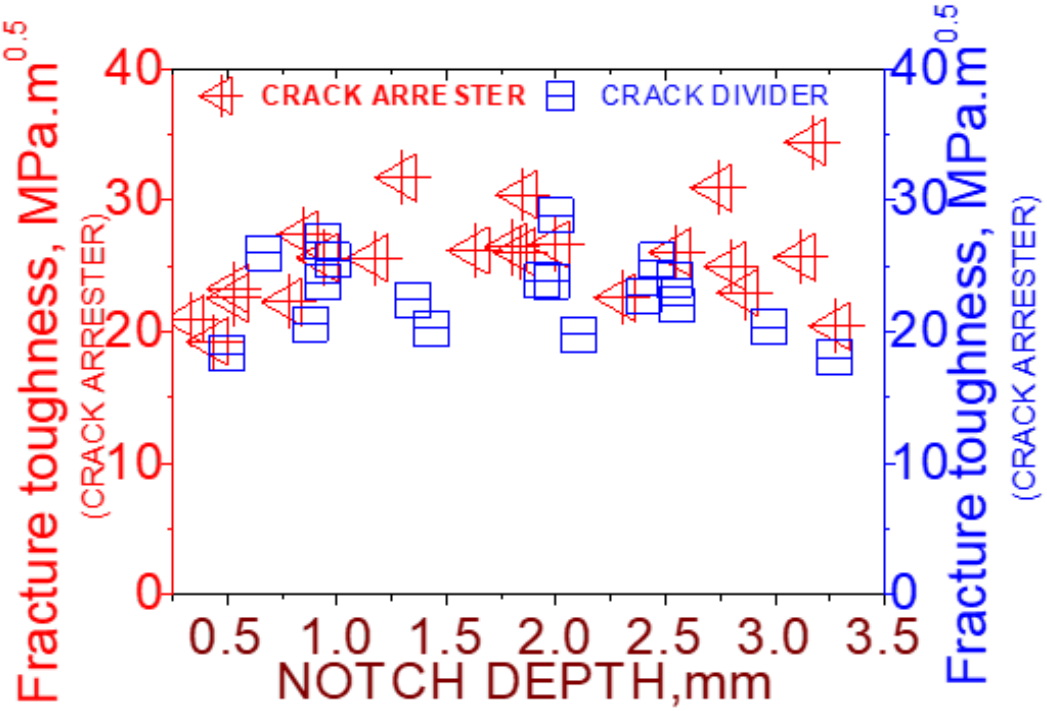

Fig. 12: Variation of conditional Fracture toughness as a function of single edge notch depth for both crack arrester and crack divider mode (irrespective of cross head speed).

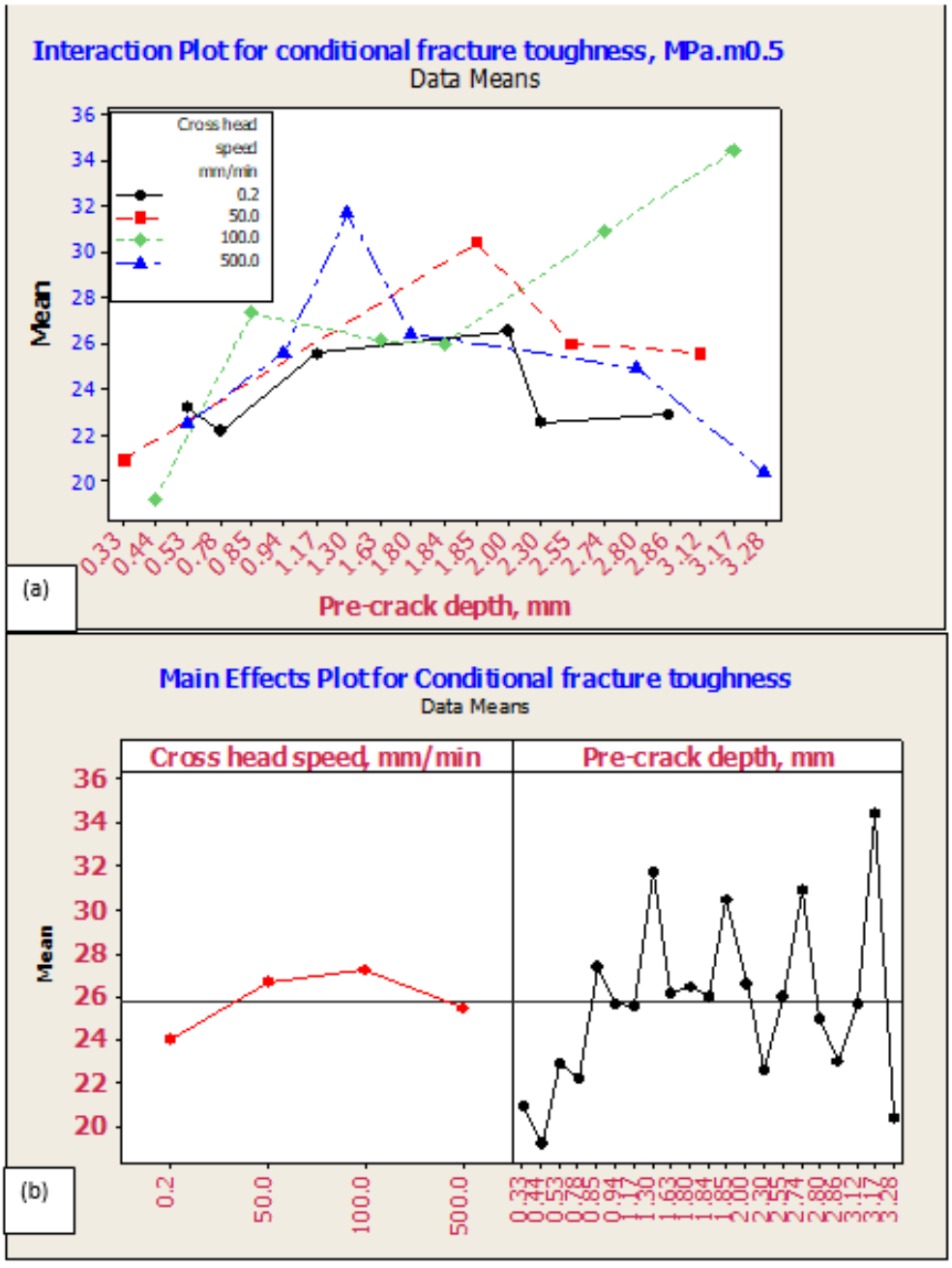

Fig. 13: (a) interaction plot and (b)main effect plot of conditional fracture toughness as a function of cross head speed and pre-crack notch depth in Crack arrester mode.

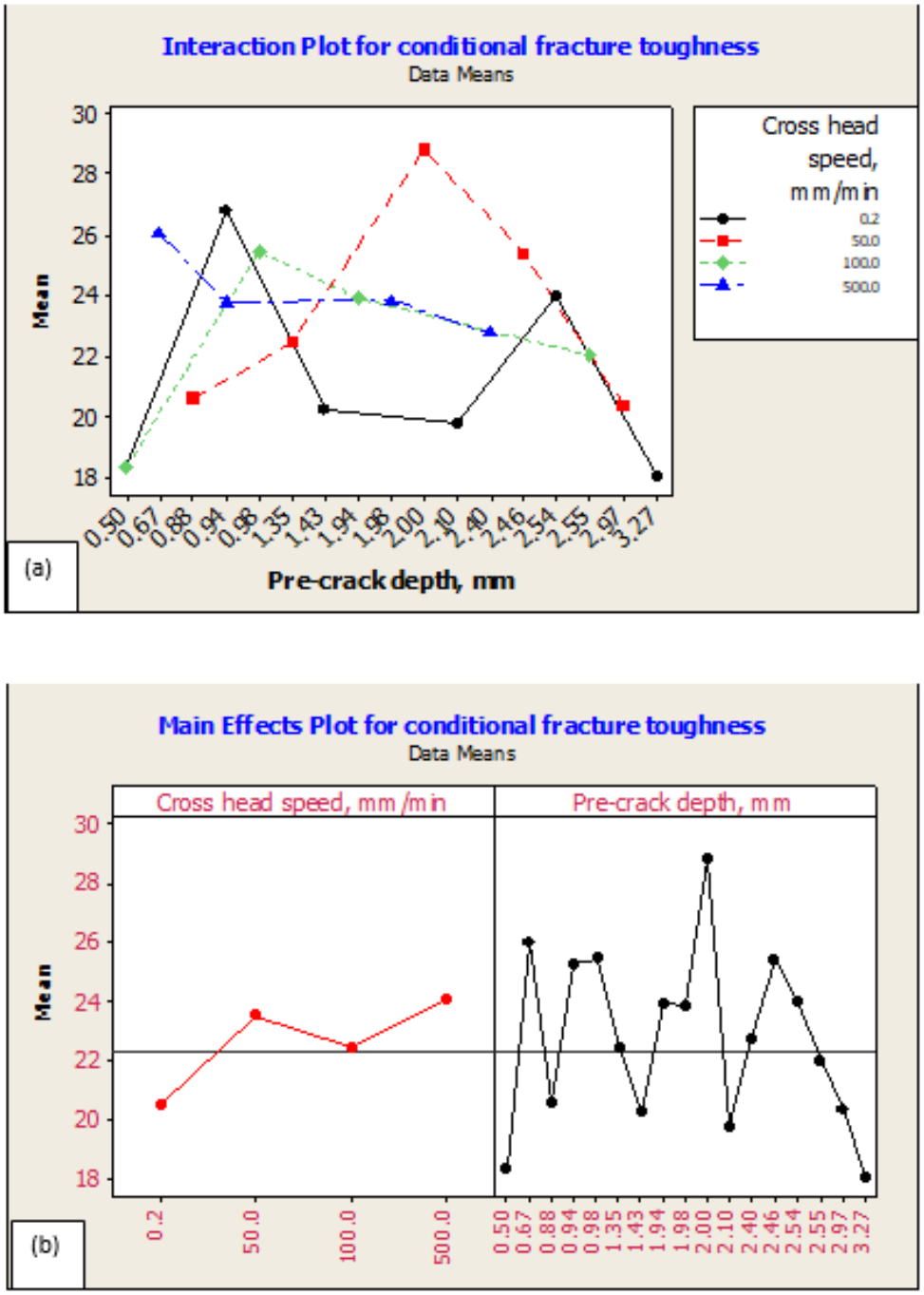

Fig. 14: (a) interaction plot and (b) main effect plot of conditional fracture toughness as a function of cross head speed and pre-crack notch depth in Crack divider mode.

3.2. Charpy Impact Test

The Impact energy of carbon epoxy composite is found to be significantly dependent on the notch depth initially at a notch depth range from 0-2 mm for the sample tested in both crack arrester and crack divider mode at room temperature. However at greater notch depth, the impact energy reached plateau for both the modes. For a constant notch depth, impact energy is found to be significantly lower in case of test in crack divider orientation than that in case of crack arrester orientation. The effect of notch depth on impact energy of the composite tested for both the modes are shown in Fig. 15.

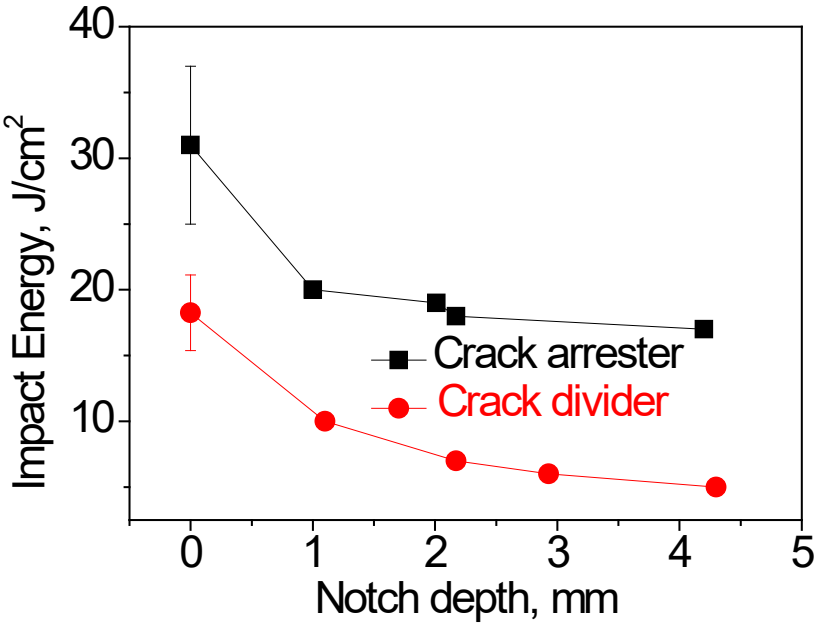

Fig. 15: Effect of notch depth on impact strength of the composite tested in crack arrester and crack divider mode at room temperature.

The photographs of the samples after charpy impact test for both the modes are shown in Fig. 16(a). While numerous delamination is observed for both notched and un-notched specimens tested in crack arrester mode, a fewer delamination is only observed for the un- notched specimens tested in crack divider mode. Delamination is rarely observed for the notched samples tested in crack divider mode. It is interesting to note here that, more number of delaminated layer is observed in case of un-notched specimens than those observed in case of notched specimen. Although not clearly established, the number of delaminated layer has clear correlation on the impact strength of the composite which constitute the further areas of research. In fact it can be clearly understood that the specimen abosorbed more energy by multiple delamination (in case of crack arrester mode), than that absorbed by breaking of carbon fibre which is predominantly observed in case of sample tested in crack divider mode as shown in Fig. 16(b). Photographs of un-notched and notched impact tested samples at -40°C are shown in Fig. 16(c) and (d). In this case also, while photographs at the left side, tested in crack arrester mode, are predominantly failed by multiple delamination, those in the right side, tested in crack arrester mode, are predominantly failed by carbon fibre breaking.

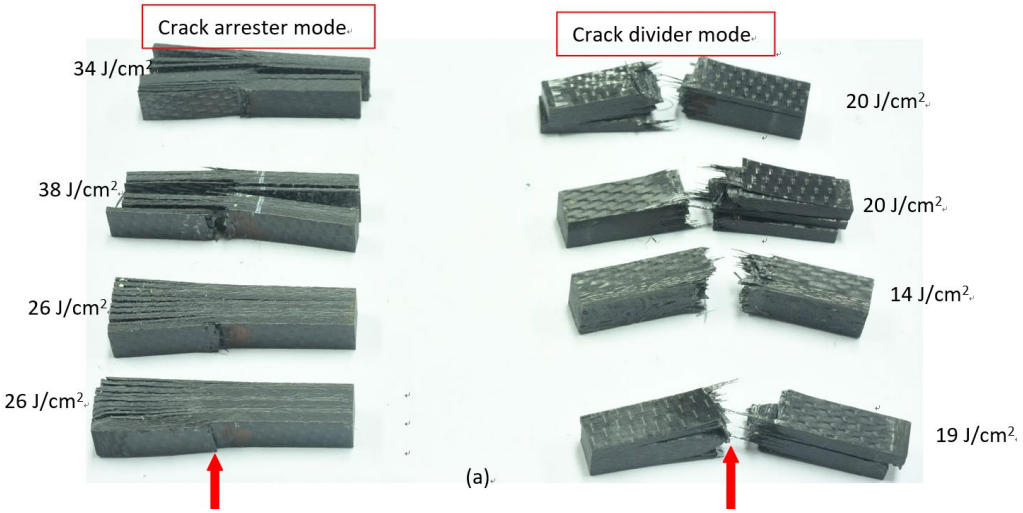

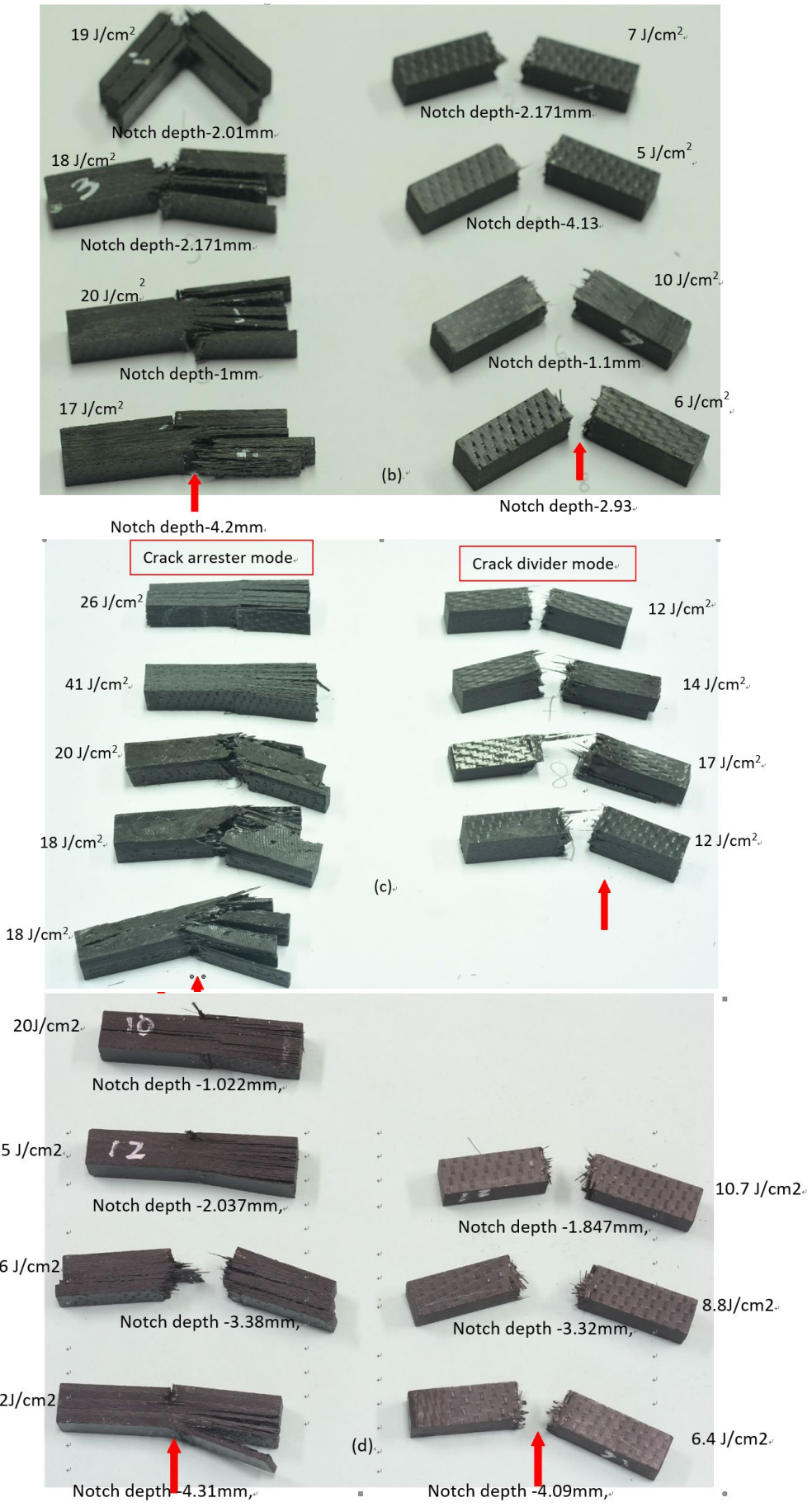
19 J/cm2
Notch depth-2.01mm
7 J/cm2
Notch depth-2.171mm
18 J/cm2
Notch depth-2.171mm
5 J/cm2
Notch depth-4.13
20 J/cm2
Notch depth-1mm
10 J/cm2
Notch depth-1.1mm
17 J/cm2
Notch depth-4.2mm
(b)
6 J/cm2
Notch depth-2.93
Crack arrester mode
Crack divider mode
26 J/cm2
41 J/cm2
20 J/cm2
18 J/cm2
18 J/cm2
12 J/cm2
14 J/cm2
17 J/cm2
12 J/cm2
(c)
20J/cm2
Notch depth -1.022mm,
15 J/cm2
Notch depth -2.037mm,
16 J/cm2
Notch depth -3.38mm,
16.2J/cm2
Notch depth -4.31mm,
10.7 J/cm2
Notch depth -1.847mm,
8.8J/cm2
Notch depth -3.32mm,
6.4 J/cm2
(d)
Notch depth -4.09mm,

Fig. 16: Photographs of room temperature impact tested samples (a) without notch (b) with different notch depth. Photographs at left sides are tested in crack arrester mode while those in the right side are tested in crack divider mode. Red arrow shows the direction of impact by hammer. Impact energy of the individual sample is also mentioned near each sample. Photographs of impact tested samples -40°C (c) without notch (d) with different notch depth. Photographs at left sides are tested in crack arrester mode while those in the right side are tested in crack divider mode. Red arrow shows the direction of impact by hammer. Impact energy of the individual sample is also mentioned near each sample

Impact energy of the samples tested at -40°C is observed to be slightly lower than that at room temperature (RT) as shown in Fig. 17. However, impact energies of the samples (RT and at -40°C) tested in crack divider orientation are significantly lower than those tested in crack arrester orientation. The Impact energy of carbon epoxy composite is found to be significantly dependent on the notch depth for the sample tested in crack divider mode at - 40°C. However impact energy significantly decreases initially at a notch depth range from 0- 2 mm with increase in depth and then reached plateau for the sample tested in crack arrester mode at -40°C. For a constant notch depth, impact energy is found to be significantly lower in case of test in crack divider orientation than that in case of crack arrester orientation. The effect of notch depth on impact energy of the composite tested for both the modes are shown in Fig. 17.

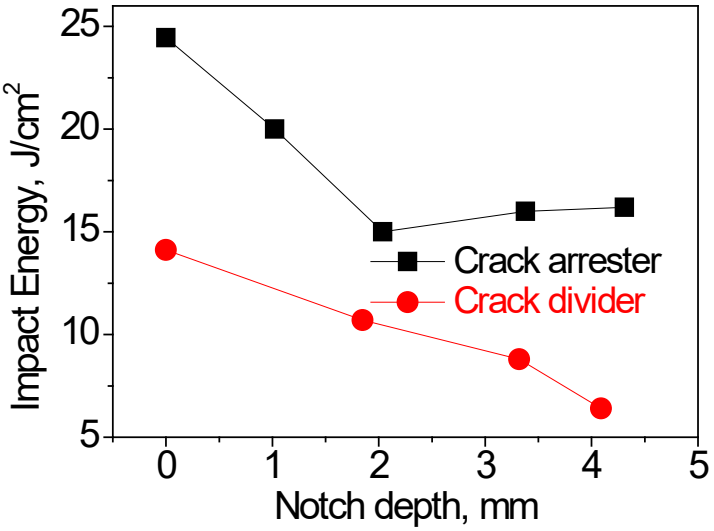

Fig. 17: Effect of notch depth on impact strength of the composite tested in crack arrester and crack divider mode at -40°C.

4. Discussion

The carbon epoxy composite samples with or without notch were subjected to three point bending load. Nature of stress on the un-notched samples subjected to three point bending load is schematically shown in Fig. 18.

4.1. Un-notched samples

In case of un-notched sample maximum tensile force acts on the bottom surface right below Load 1. In case of crack divider mode, this tensile force causes breaking of the bottom/near bottom carbon fibres which are oriented parallel to line B. However, breakage of the carbon fibre at the bottom surface with orientation parallel to Line B will be governed by the failure of the weakest link. As is shown in Fig. 19 that the diameter of individual carbon fibre vary slightly along its length and the diameter of all the carbon fibre are not same. This difference causes different fibres to break at different heights (as shown in Fig. 20). Therefore, crack does not get generated exactly along line M below the load 1 and does not get propagated exactly parallel to line L. Rather, crack path becomes highly tortuous. These tortuous crack propagations may or may not initiate notch between the carbon fibre lamina in case of crack divider orientation. Therefore, delamination is rarely seen (Fig. 9) in case of crack divider mode.

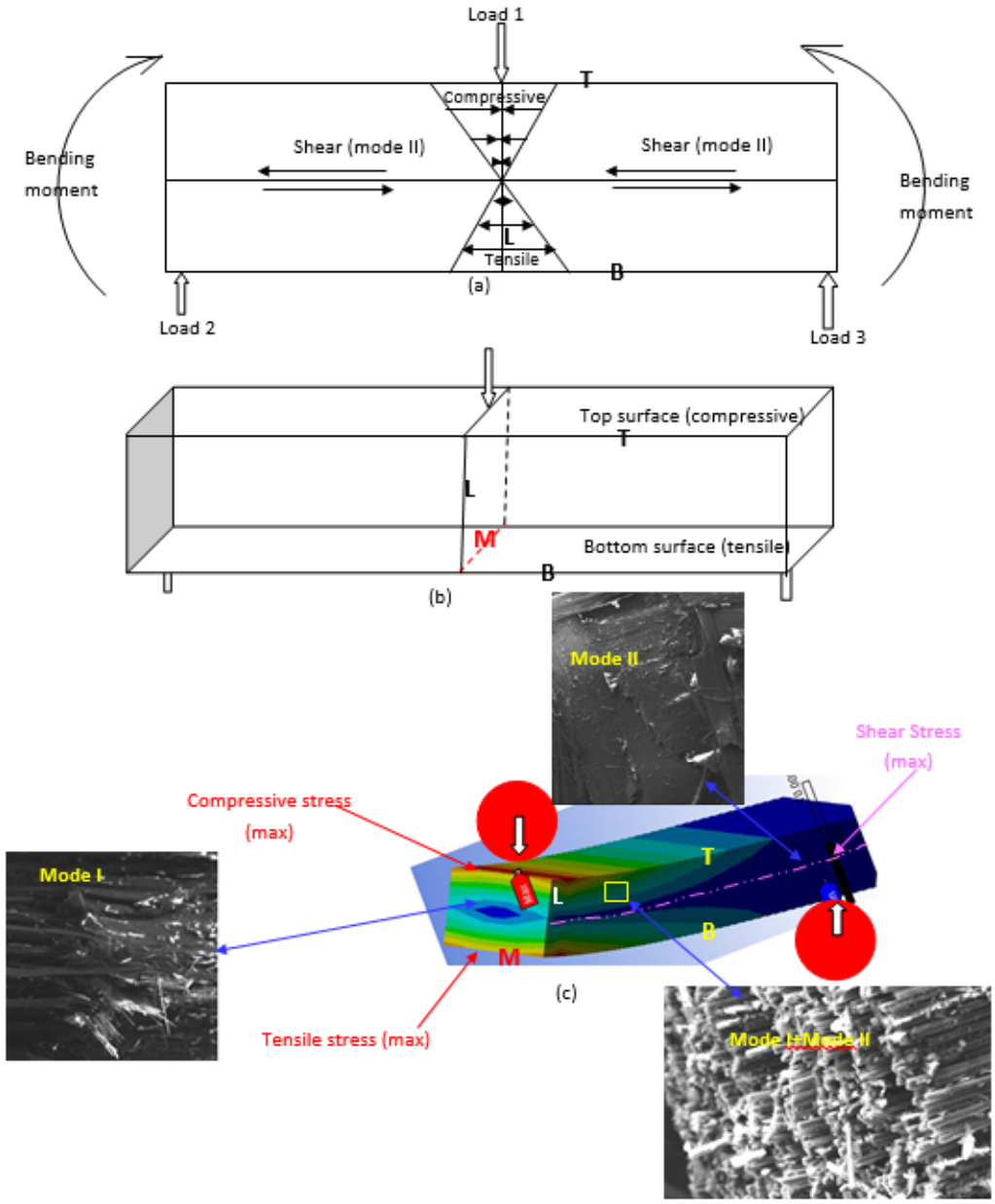

Fig. 18: Shows (a) two dimensional and (b) three dimensional schematic diagram and (c) stress distribution (from ANSYS 15.0) on the un-notched samples subjected to three point bending load. Line M and L are shown in these Fig.s to facilitate discussion. Typical mode I, Mode II and mixed mode fracture location with typical microstructure after failure in crack divider mode is also shown in (c).

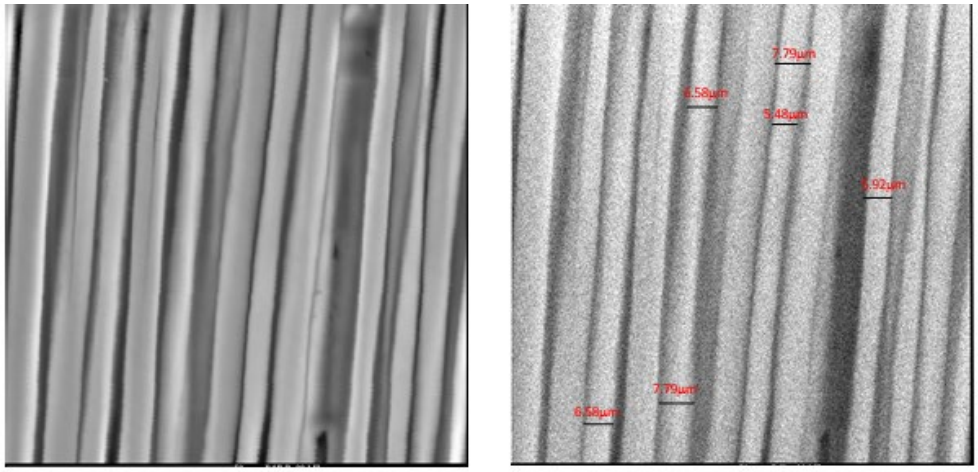

Fig. 19: (a) BSE image and (b) carbon maps for carbon epoxy composite, There is a slight variation of diameter of different carbon fibres, variation of diameter is also seen for same carbon fibres along its length.

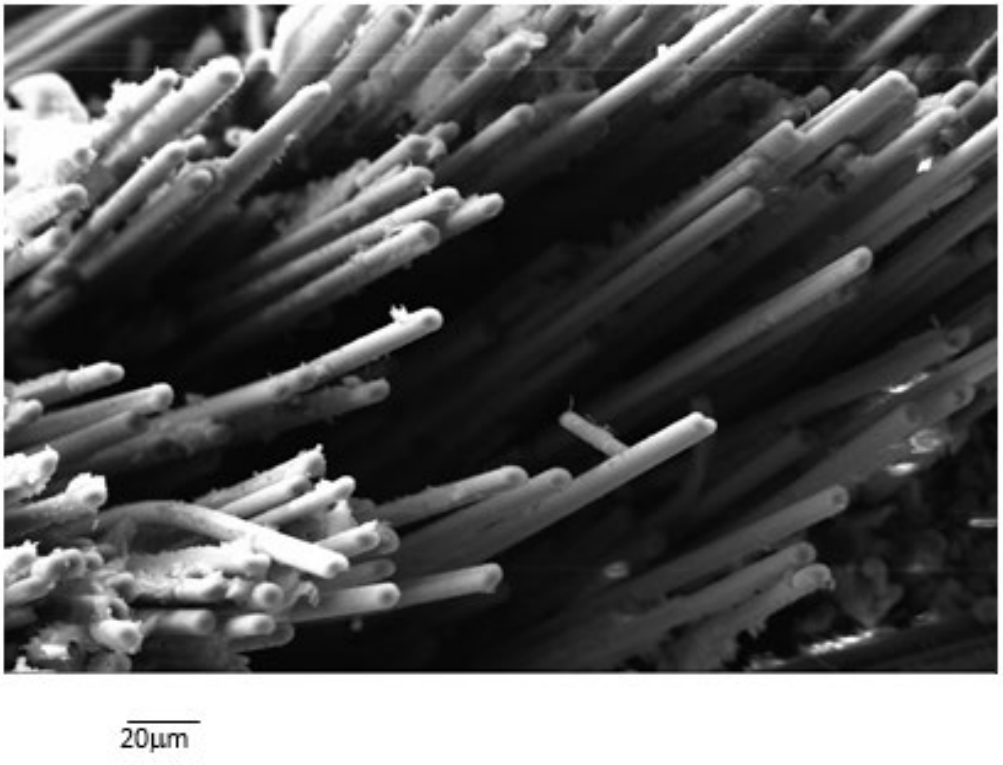

Fig. 20: fibres, which are parallel to line B and are situated near bottom side of the 3-point bend tested specimen, break at different heights are governed by the failure of the weakest link.

On the other hand, the top/near top carbon fibres which are oriented parallel to line T experience compressive force which cause breaking by twisting of the carbon fibres. However, the carbon fibre or bunch of carbon fibre which are oriented parallel to Line L will not experience tensile force, rather they experience shear force. This shear force causes clock wise bending of the bottom part of these fibres which are on the left side of L and anti-clock wise bending of the bottom part of these fibres which are on the right side of L. A low magnification Fracture surface of unnotched samples 3 point bend tested in crack divider mode at a cross head speed of 500 mm/min is shown in Fig. 21 in order to visualize the carbon fibre fabrics and their mode of fracture at different locations and orientations as well as crack propagation direction. The fractograph shows tensile fracture near bottom surface and compressive fracture near top surface of the bunch of fibres which are parallel to line B and T respectively. Fibres parallel to line L is apparently seen to be unaffected in lower magnification. From the tensile and compressive fracture region (red rectangles, Fig. 21), a rough estimation of crack propagation direction is also shown in Fig. 21 by red thick arrow.

A relatively closer view of the region near bottom surface is also shown separately in Fig. 20. The bunch of carbon fibres (in the fabric/lamina) which are parallel to line B are fractured by tension which is substantiated by cup and cone fracture of the fibres (Fig. 22 c). On the other hand, the bunch of fibres which are parallel to Line L, are subjected to shear force, bend and come out above the fracture plane. Evidence of breaking of some of the fibres of this bunch are also seen due to bending cause by the shear force (Fig. 22 b). A relatively closer view of the region near top surface is also shown separately in Fig. 23. The bunch of fibre parallel to line T are fracture in this region (read rectangle Fig. 23a) by compression which is substantiated by bending and breaking fracture (c). The bunch of fibres parallel to Line L are subjected to shear force, bends and breaks. Tensile and compression side of the bend fibre is marked in (c). In case of crack divider mode the carbon lamina is placed vertically and thus crack initiation at the bottom surface is relatively easy and crack propagation is difficult since in this mode the event of initiation of notch in between the lamella during crack propagation along Line L is relatively difficult. Therefore falling of load is not as steep as that in case of crack arrester mode. Further, slight load rise is observed occasionally in the event of interlamellar separation (Fig. 11).

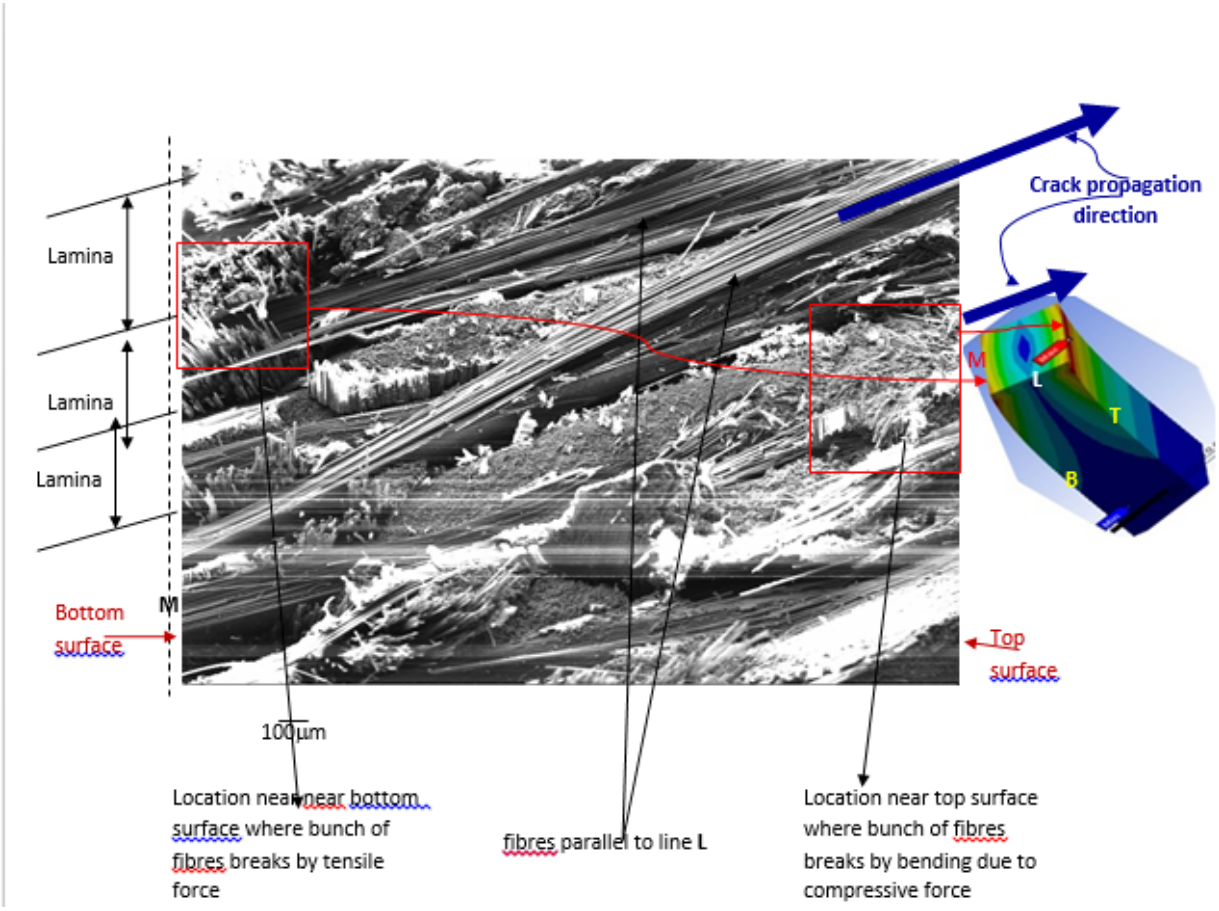

Fig. 21: A low magnification SEM fractographs of the 3 point bend tested sample without notch in crack divider mode at 500mm/min cross head speed. The fractograph shows tensile fracture near bottom surface and compressive fracture near top surface of the bunch of fibres which are parallel to line B and T respectively. Fibres parallel to line L is apparently seen unaffected in lower magnification.

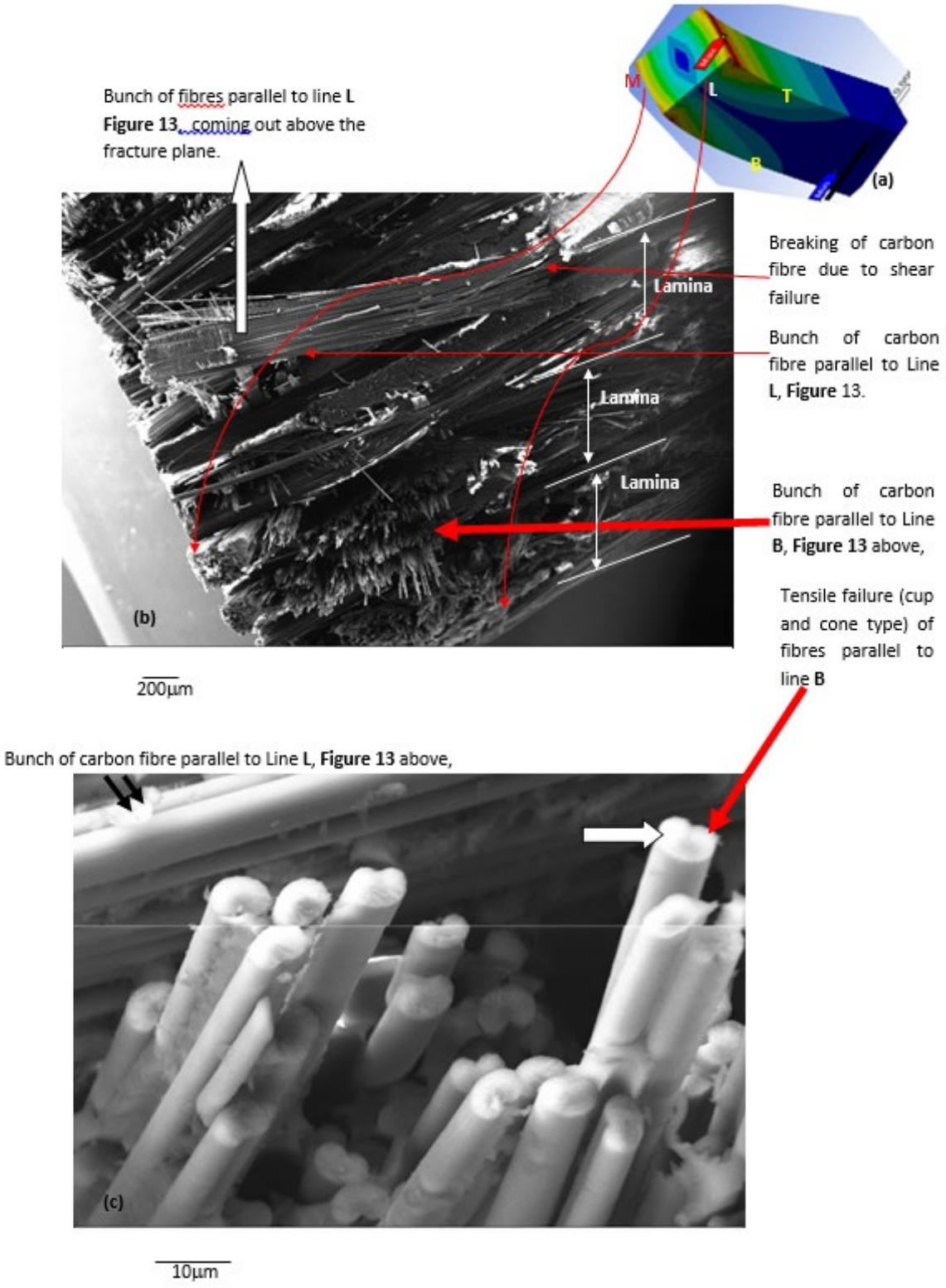

Fig. 22: (a) Schematic of 3 point bend tested sample and (b) fracture surface of unnotched samples 3 point bend tested in crack divider mode at a cross head speed of 500 mm/min. The bunch of fibre parallel to line **B** are fracture by tension which is substantiated by cup and cone fracture (**c**). The bunch of fibres parallel to Line **L** are subjected to shear force, bends and come out above the fracture plane. Some of these fibres breaks due to bending caused by the shear force.

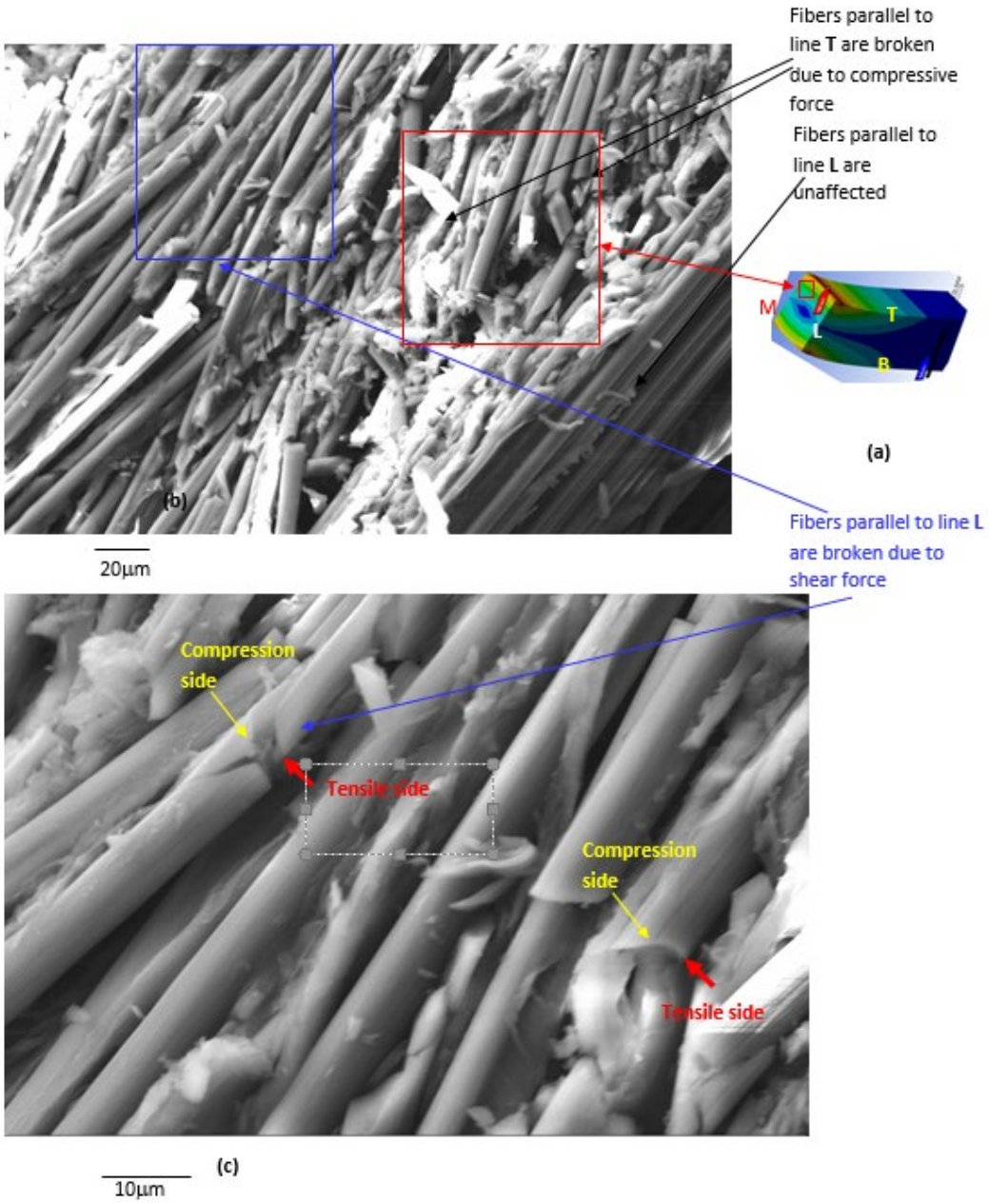

Fig. 23: (a) Schematic of 3 point bend tested sample and (b) fracture surface of unnotched samples 3 point bend tested in crack divider mode at a cross head speed of 500 mm/min. The bunch of fibre parallel to line **T** are fracture by compression which is substantiated by bending and breaking fracture (**c**). The bunch of fibres parallel to Line **L** are subjected to shear force, bends and breaks. Tensile and compression side during fibre bending is marked in (c).

In case of crack arrester mode (as schematically shown in Fig. 4), this tensile force causes breaking of carbon fibre or bunch of carbon fibre which are oriented parallel to line B and causes no breaking of fibres which are oriented parallel to line M as shown in Fig. 24a. Although most the fibre which are oriented parallel to line B are broken due to tensile force, higher magnification image shows some of the fibre are broken due to bending during 3 point bend test (Fig. 24b). In this mode there is no carbon fibre exist parallel to Line L. In this mode also, breakage of the carbon fibre at the bottom surface with orientation parallel to Line B will be governed by the failure of the weakest link. Therefore, crack does not get generated exactly along a horizontal straight line perpendicular to line B right below the load 1. Furthermore, as is evident in Fig. 24, that bunch of upper fibres, which are oriented parallel to line B, are all broken and the bunch of fibres located below which are oriented parallel to line M are not at all broken. This causes crack path get slightly tilted and crack does not get propagated exactly parallel to line L, rather, crack path becomes highly tortuous. This tortuous crack propagation during 3-point bending invariably initiate notch between the carbon fibre lamina

in case of crack arrester orientation. This causes delamination to take place by mode II in case of crack arrester mode as seen in Fig. 8a.

It is important to note here that, maximum load for un-notched sample in case of crack arrester mode is substantially higher than that in case of the crack divider mode (Refer Fig. 10 and 11). This is because of the fact that, in case of crack arrester mode, the carbon fibre fabric (lamina) is placed horizontally and thus crack initiation at the bottom surface is very difficult. However, once crack gets initiated, its tortuous propagation easily initiate notch between the carbon fibre lamina. Therefore, the load drops sharply and again rises slightly because of subsequent propagation of crack in between the lamellae by delamination. Interlamelar separation of delamination is mainly caused by shearing (mode II) as shown by Fig. 18. The shearing (mode II) failure is substantiated by the cusps morphology (Fig. 25 b). The delamination is caused by the crack propagation through interface or matrix failure as shown in Fig. 25. The morphology of cusps and river marking gives good indication of direction of crack propagation. Direction of crack propagation is marked in Fig. 25 by red arrow. Although shearing force (mode II) only cause interface and matrix separation, sometimes this shearing force breaks or bend the carbon fibres also. If carbon fibres are oriented parallel to shearing direction, the bunch of fibres bend as shown in Fig. 26. Shearing force also breaks the carbon fibres which are perpendicular the shearing force as shown in Fig. 27.

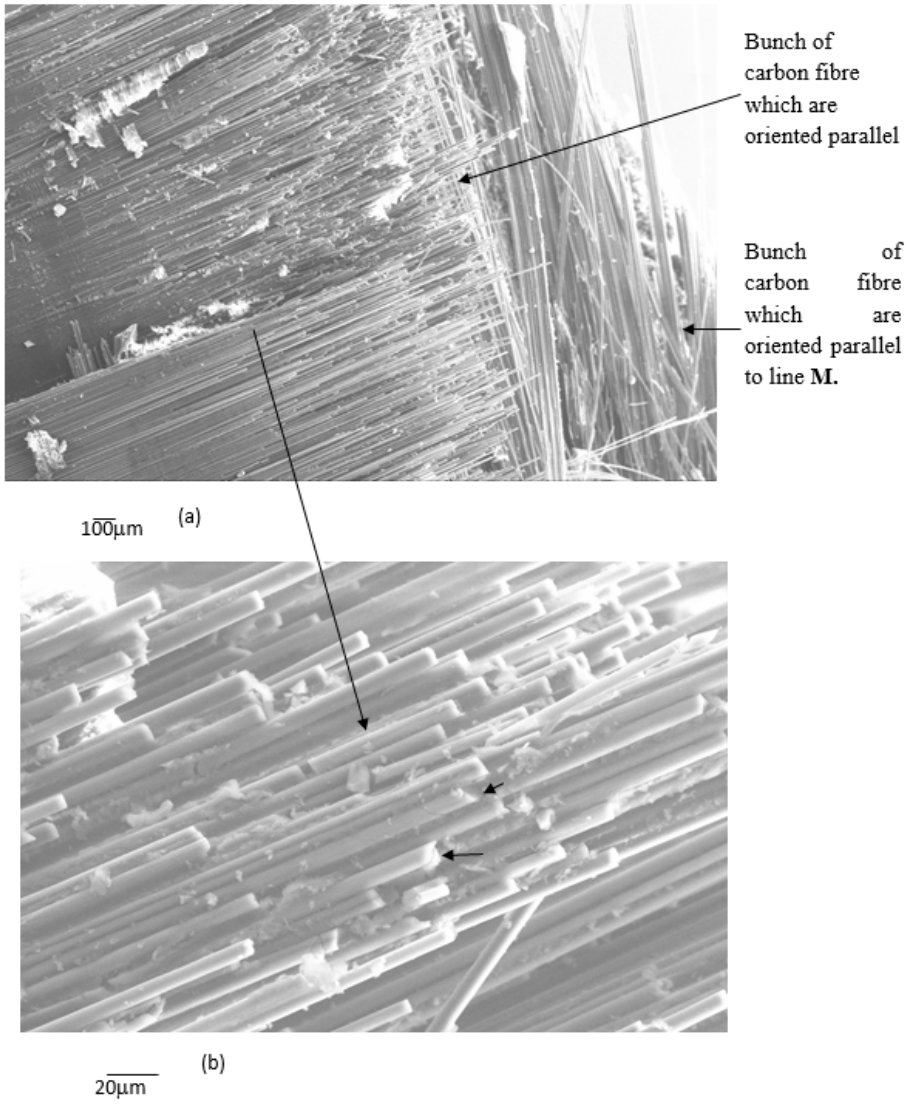

Fig. 24: (a) SEM low magnification image of the fracture surface of 3-point bend tested sample tested in crack arrester mode. The tensile force cause breaking of bunch of carbon fibre which are oriented parallel to line **B** and causes no breaking of fibres which are oriented parallel to horizontal straight line perpendicular to line **B.** (b) higher magnification image shows although most the of fibres fail by tensile force, some are also broken by bending force (marked by black arrow)

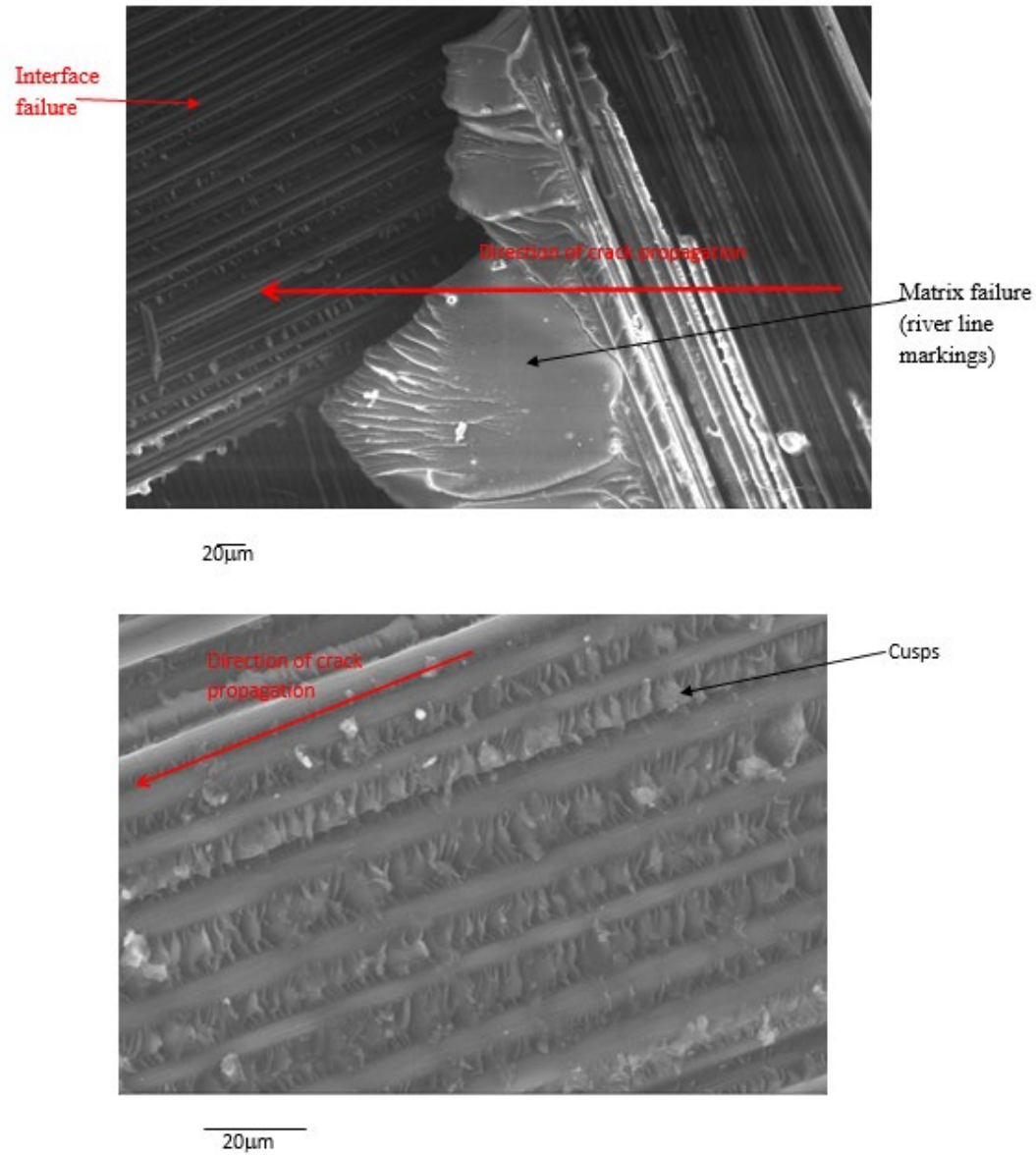

Fig. 25: (a) SEM image of delaminated surface. Interlamelar separation of is mainly caused by shearing (mode II) as shown by Fig. 13. Delamination is caused by crack propagation because of interface or matrix failure. (b) SEM image of cusps morphology.

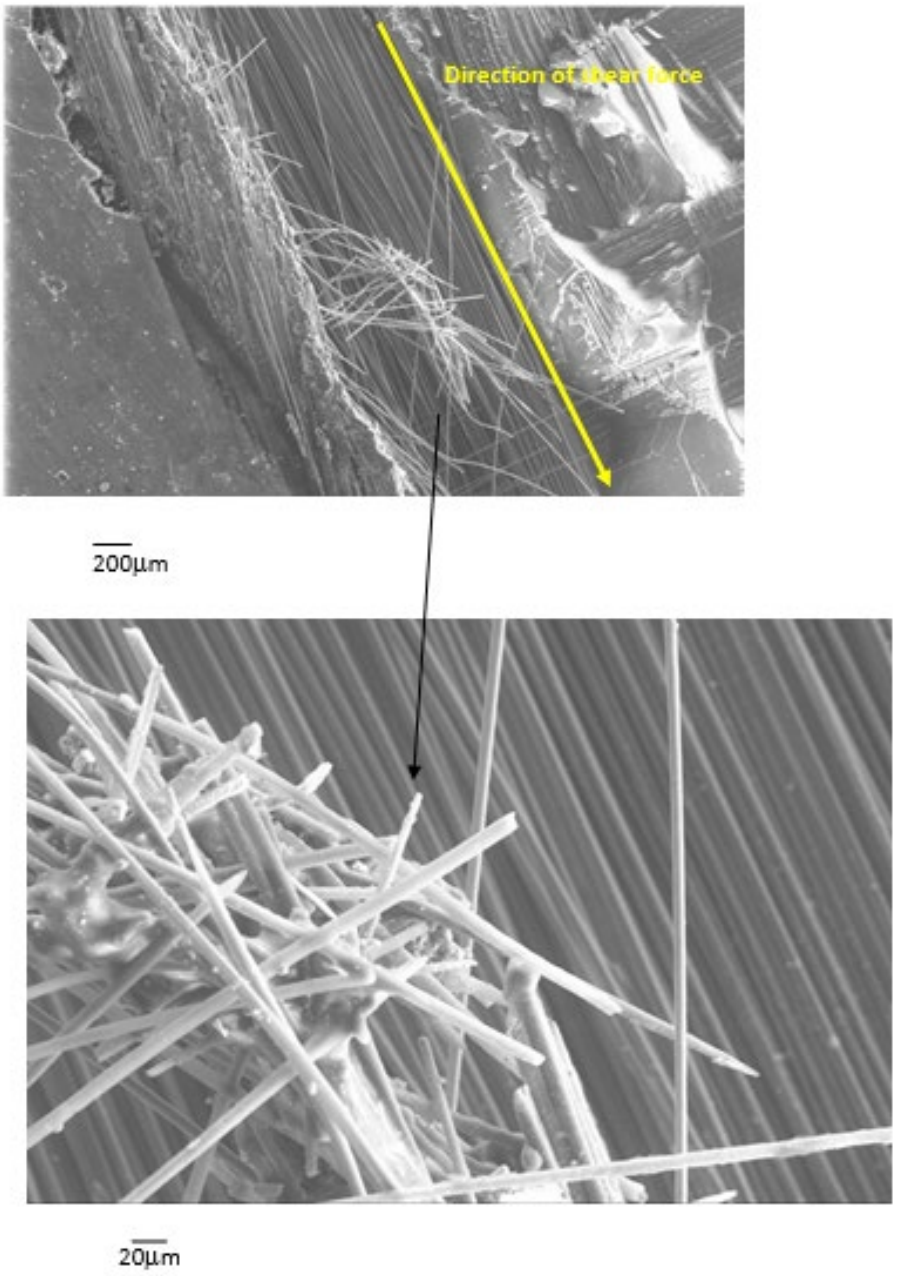

Fig. 26: (a) bending of the bunch of fibres oriented parallel to shearing direction (b) higher magnification SEM image.

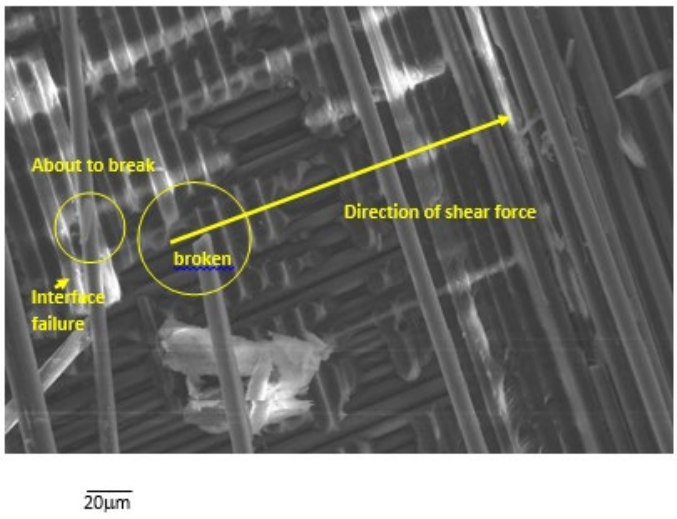

Fig. 27: Shearing breaks the fibres which are oriented perpendicular to the direction of shear.

4.2. Pre-crack notched samples

From the stress concentration analysis using ANSYS 15.0 (Fig. 28) it is observed the higher the notch depth, the lower overall stress/applied stress required to obtain 650MPa (flexural strength of the composite) stress at the crack tip.

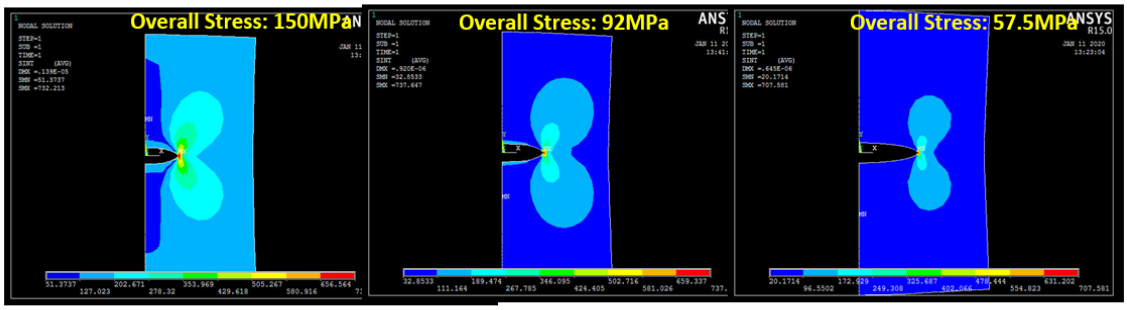

Fig. 28: ANSYS calculation shows that the combination of overall/applied stress and the notch depth, required for obtaining 650MPa (flexural strength of the composite) stress at the crack tip.

On the other hand, it can be said that the higher the notch depth, the higher is the stress concentration at the crack tip. This is well explained in Fig. 29 where it is clearly seen that the F(α) (geometric factor, function of notch depth) increases sharply when the pre-crack notch depth exceeds certain value.

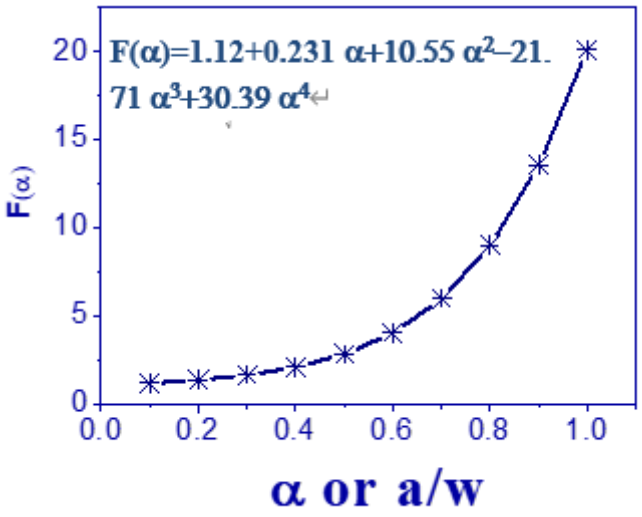

Fig. 29: Variation of F(α) with notch depth

In crack arrester mode, at lower notch depth specimens fail by single layer delamination by shear (mode II) and conditional fracture toughness is observed to be lower. As the notch depth increases, specimens fail by multiple delamination by shear (mode II). Therefore at intermediate notch depth, conditional fracture toughness is higher. However, at very high notch depth stress concentration at the crack tip is sufficient to cause breaking of bunch of carbon fibre. This causes pure Mode I failure and therefore conditional fracture toughness is again low and becomes equal to K1c. In crack arrester mode this value is found to be 20.4MPa.m0.5 (**Table 1**). A separate set of experiments is carried out to ensure pure mode I failure for both the mode of test (**Fig. 30**). This has also proves that the K1c is equal to 20.4MPa.m0.5 which is similar to reported value in the literature.

In crack arrester mode, it is interestingly observed that modulus decreases with the notch depth. As the notch depth increases amount of delamination observed to be more which causes decrease in modulus. As the higher cross head speed favours delamination (mode II) modulus decreases at higher cross head speed. In crack divider mode, crack has to propagate by breaking bunch of fibres only which is difficult at lower and intermediate notch depth. Therefore, modulus does not change much with crack depth.

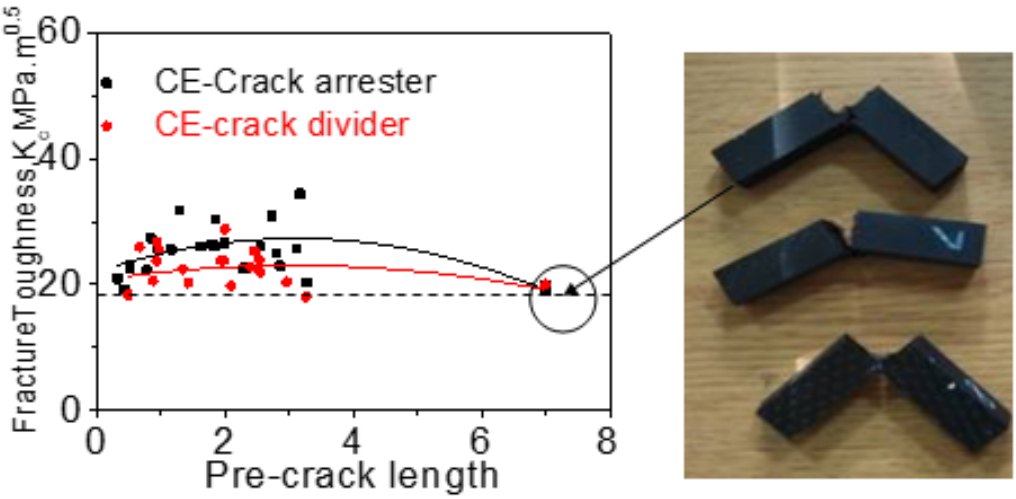

Fig. 30: pure mode I failure for the composite. K1Cis approximately equal to 20 MP a.m0.5.

In case of single edge notched specimen the schematic stress distribution during three point bend test is schematically shown in Fig. 31. The maximum tensile stress is observed at the crack tip. This tensile stress is responsible for carbon fibre breaking.

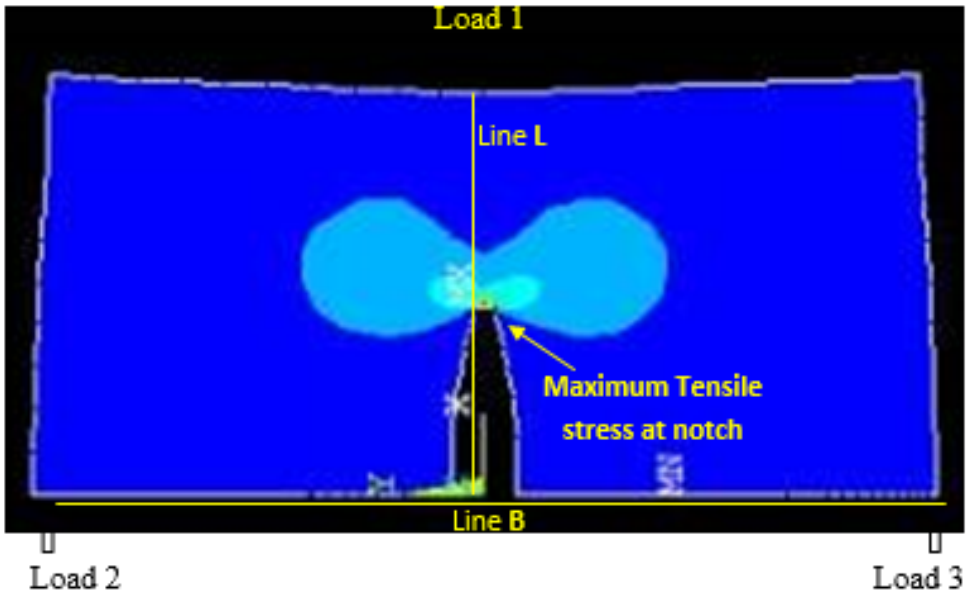

Fig. 31: Schematic of Stress distribution of single edge notch beam during three point bend loading. Maximum tensile stress is at the crack tip.

In notched samples, maximum tensile force acts at the crack tip right below Load 1. In case of crack divider mode (as schematically shown in Fig. 5c-d), this tensile force causesbreaking of the crack tip carbon fibres which are oriented parallel to line B, Fig. 31. However, Fibres which are aligned parallel to Line L, Fig. 31 will not experience any tensile force hence will not fail (yellow double arrow, Fig. 32). Fig. 32a,b shows SEM image near the crack tip of the samples which were having a notch depth of 0.5mm and were 3-point bend tested at 0.2mm/min and 50mm/min cross head speed respectively. Both the fractographs show that the fibres parallel to the line L (shown by yellow arrow) remain unaffected, while the fibres parallel to line B (shown by double yellow arrow) are broken. Tip of the broken fibres of Fig. 32b are found to be hemispherical indicating that the fibres are broken due to action of tensile force.

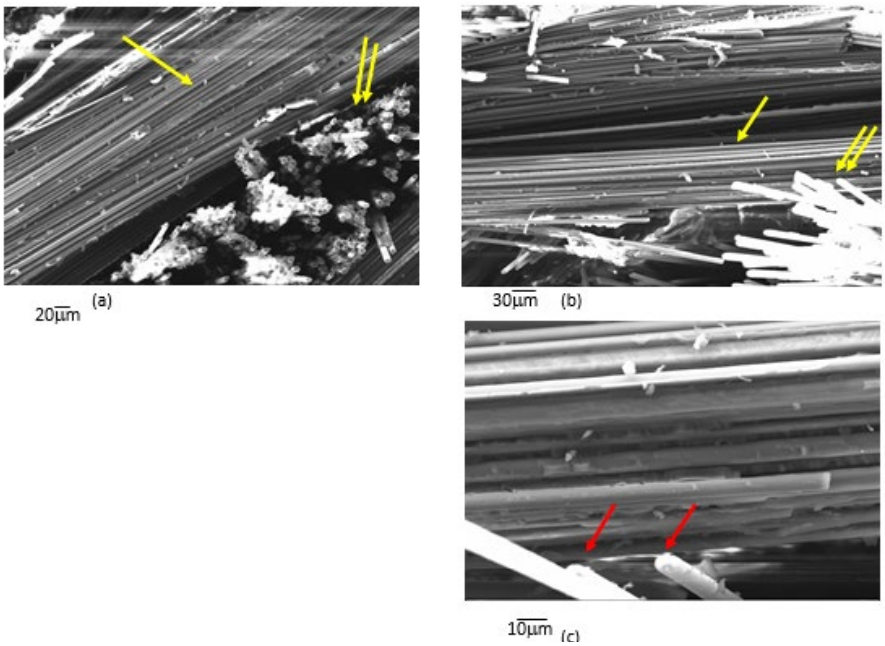

Fig. 32 : Fractographs at the crack tip of the samples having 0.5mm notch depth, 3-point bend tested at (a) 0.2mm/min and (b) 50mm/min cross head speed. Both shows that the fibres parallel to the line **L** (shown by yellow arrow) remain unaffected, while the fibres parallel to line B (shown by double yellow arrow) are broken. Tips of the broken fibres (red arrow) in Fig. 24b are hemispherical indicating tensile cup and cone fracture.

Unlike in the case un-notched samples, for notched samples which are tested in crack divider mode, intense tensile stress develop at the crack tip only **(Fig. 31)** most of the fibres which are parallel to line **B** will break at the same height (**Fig. 32a)** although some fibres still break at different heights also (as shown in **Fig. 32c**). This makes crack path less tortuous than that in case of un-notched sample. From Load vs. Displacement curves in Fig. 11 also it is observed that failure of un-notched sample are relatively gradual than that of the notched samples.

Notched samples which are tested in crack arrester mode, intense tensile stress develop at the crack tip only **(Fig. 31).** Most of the fibres which are parallel to line **B** break at the crack tip **(Fig. 33)** and the crack propagates tortuous way along the line **L.** This tortuous crack path causes nucleation of interlamellar cracks. For notch depth of 2.5 mm, mostly opening mode (mode I) predominates and crack prefers to propagates tortuous way along the line **L** without causing much delamination**.** However, for notch depth below 2.5mm, crack propagates both by mode I (opening mode) and mode II (shearing mode). In this case tortuous crack propagation along line **L** causes nucleation of interlamellar cracks which propagate and culminate into delamination as shown in **Fig. 34.** Crack propagation direction for mode II (delamination) is marked in **Fig. 34.** It is important to note here that delamination is characterized by stick-slip behaviour which rise and drop of load with respect to displacement.

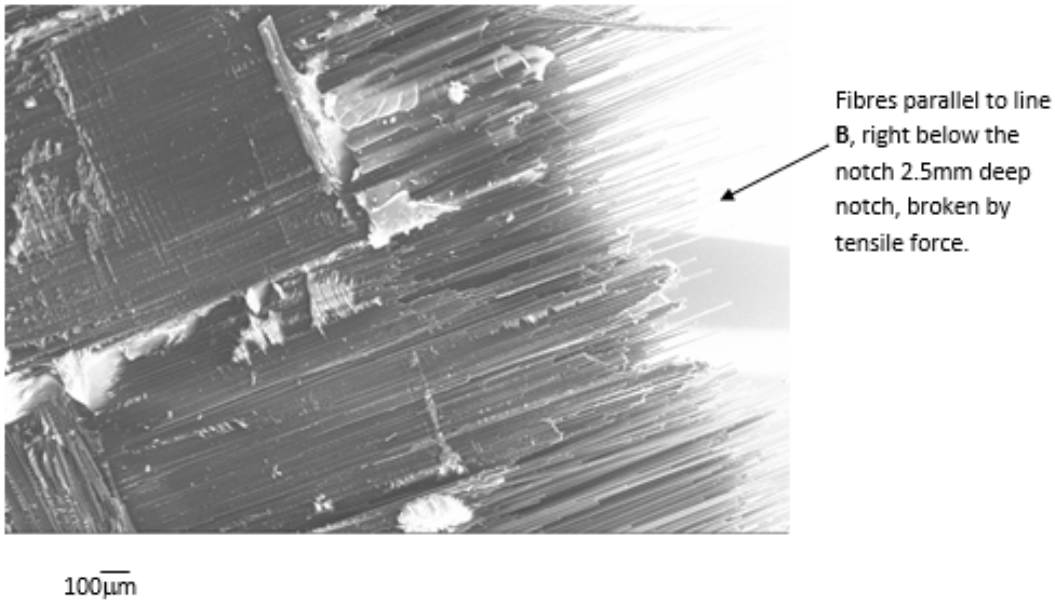

Fig. 33: SEM image of Fibres parallel to line **B**, right below the notch 2.5mm deep notch, broken by tensile force after three point bend tested at 50mm/min cross head speed in crack arrester mode.

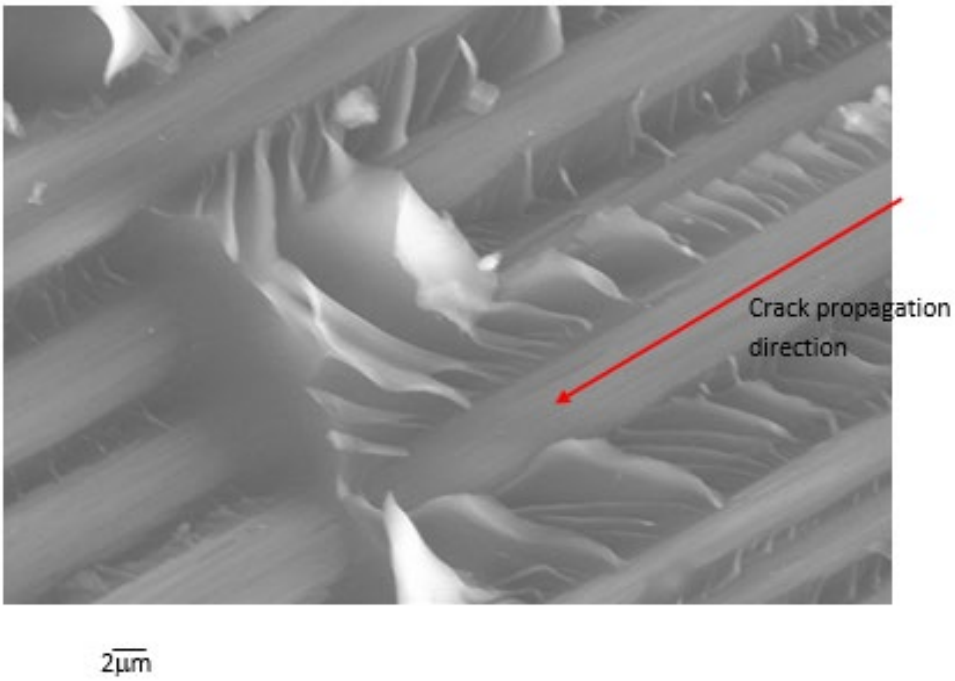

Fig. 34: SEM image of typical delamination observed in carbon epoxy composite 3-point bend tested in crack arrester mode**.** Crack propagation direction for mode II (delamination) is marked with red arrow**.**

It is important to note here that delamination is characterized by stick-slip behaviour which is the rise and drop of load with respect to displacement. This stick slip behaviour is maximum for load displace curves for the 3 point bend tested samples with notch depth 1.5mm (Fig. 10) which corresponds to delamination dominated (mode II) failure. This fact is substantiated by the fact that failed samples with 1.5mm notch depth show multiple delamination. Although the correlation between the cross head speed on the extent of delamination is not clearly established in this study, it is clearly observed in this study that higher cross head speed (500mm/min) during 3-point bend test in crack arrester mode favours multiple delamination (Fig. 8c and d). This apparently points toward the fact that the interlaminar fracture toughness seems to decrease with loading rate. Effect of loading rate on Mode II interlaminar fracture toughness by the other researchers are summarized in Table 2. Except Kageyama and Kimpara [20] all the other researchers observed decrease of Interlaminar fracture toughness with increase in loading rate which corroborates our findings. Contradictory finding observed by Kageyama and Kimpara [20] may be due their experiment at very high loading rate (480000mm/min).

Table 2: effect of loading rate on mode II interlaminar fracture toughness (FT) of carbon epoxy composite.

Loading rate range	**Loading rate effect on Mode II Interlaminar fracture toughness**	**remarks**
0.2-500mm/min	Mode II Interlaminar fracture toughness seems to decrease with increasing loading rate	**Since in this study it is observed that multitple delamination is favoured by the increase in loading rate**
0.252-5520 mm/min	Mode II Interlaminar fracture toughness decreases with increasing loading rate	**Smiley and Pipes [15]**

75000-180000mm/min	Mode II Interlaminar fracture toughness decreases with increasing loading rate	**Maikuma *et al.* [16]**
0.252-5520 mm/min	Mode II Interlaminar fracture toughness decreases with increasing loading rate	**Chapman *et al.* [17]**
10^{-5} sec^{-1} to 10^{-2} sec^{-1}	Mode II Interlaminar fracture toughness decreases with increasing loading rate	**Kusaka *et al.*[18, 19]**
0-480000mm/min	Mode II Interlaminar fracture toughness increases with increasing loading rate	**Kageyama and Kimpara [20]**

Although the correlation between the cross head speed on the maximum load in the load displacement curve is not clearly established in this study. Apparently, it is observed that the higher the cross head speed, the higher is the maximum load. It is observed from the ANOVA analysis (Fig. 13 and 14) that the conditional fracture toughness of carbon epoxy composite apparently increases with the loading rate (or cross head speed). The fracture toughness (K_{1C}, $MPa.m^{0.5}$)and flexural strength obtained in this study is compared with the similar findings observed in the literature and is recorded in Table III.

Table 3: K_{1C}, Flexural strength obtained in this study vis-a-vis these properties obtained by other researchers

Sl. No.	K_{1C} $MPa.m^{0.5}$	Flexural Strength, MPa	
1	20 (both CA and CD mode)	*641±48(CA mode)* *634±49(CD mode)*	**This study**
2	26.5		**Ankita *et al.* [21]**
3	9.015		**Melten E T[22]**
4		506±16	**Dong Quan [23]**
5		304.81±14.30	**Prashanth T [24]**
6		629±39	**Alok K S [25]**
7		482.0/493.2/503.4	**Kishore S [26]**
8		799.63±51.83	**Ekramul I [27]**

4.3. Charpy Impact Test

Carbon epoxy composite favours multiple delamination at very high loading rate. This may be due to the fact that the energy dissipation is faster by multiple delamination which is required when deformation rate is higher. As the mode II interlaminar / delamination fracture toughness decreases with the loading trate (refer Table 2 above), multiple delamination is the prefer route of energy dissipation at high strain rate. This fact is clearly established by charpy impact test (strain rate 10^3/s), where deformation rate is significantly high. All the samples tested in crack arrester mode shows numerous delamination (Fig. 16). While un- notched samples fail mainly by multiple delamination (mode II) and showed higher imapct energy, notched specimen fails both by carbon fibre breaking (mode I) and delamination (mode II) and shows lower imapct energy during charpy impact test. In case of impact test in crack divider mode, while un-notched samples fail both by delamination (mode II) and carbon fibre breaking (mode I), notched specimens predominantly fail by carbon fibre breaking (Mode I). In case of impact test in crack divider mode, un-notched samples show higher impact energy than the notched specimens (Fig. 15). From this study it is clearly established that, the composite

absorbs higher impact energy when it fails purely by mode II (multiple delamination) followed by mixed mode failure. The Composite absorbs lowest impact energy when it fails by purely mode I (carbon fibre breaking). Therefore, the specimen shows significantly higher impact energy during impact test at crack arrester mode than that during impact test at crack divider orientation. The Schematic of correlation of Impact energy with the mode of failure of the composite is shown in Fig. 35. Typical SEM photographs of mode I, Mode II and mixed mode fracture surface is also shown in Fig. 36.

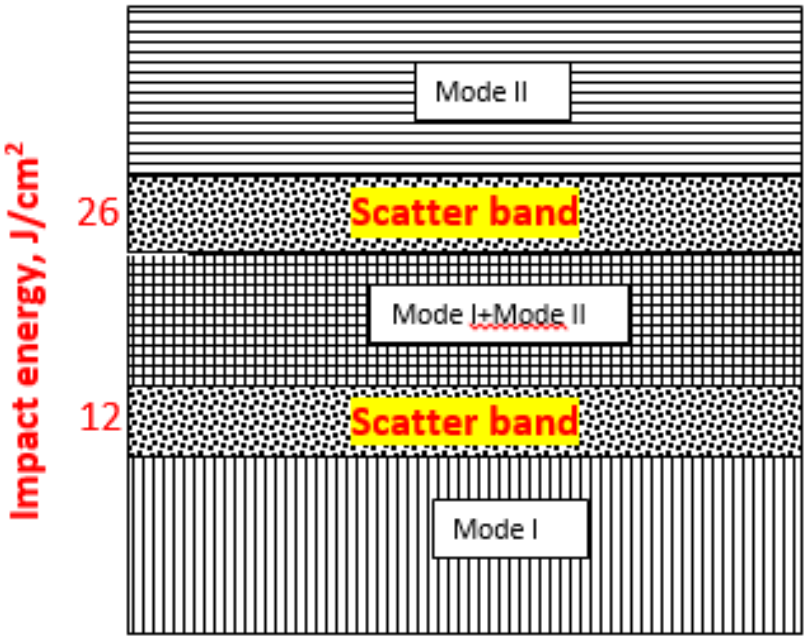

Fig. 35: Schematic of correlation of Impact energy with the mode of failure of the composite.

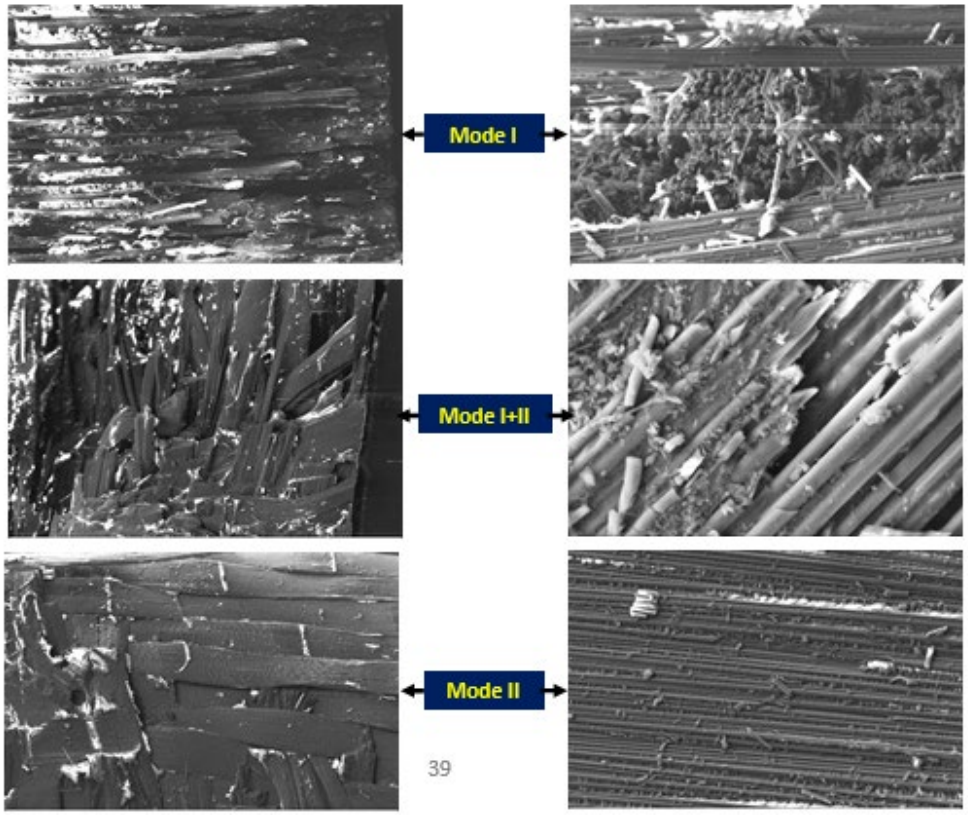

Fig. 36: Typical SEM photographs of mode I, Mode II and mixed mode fracture surface.

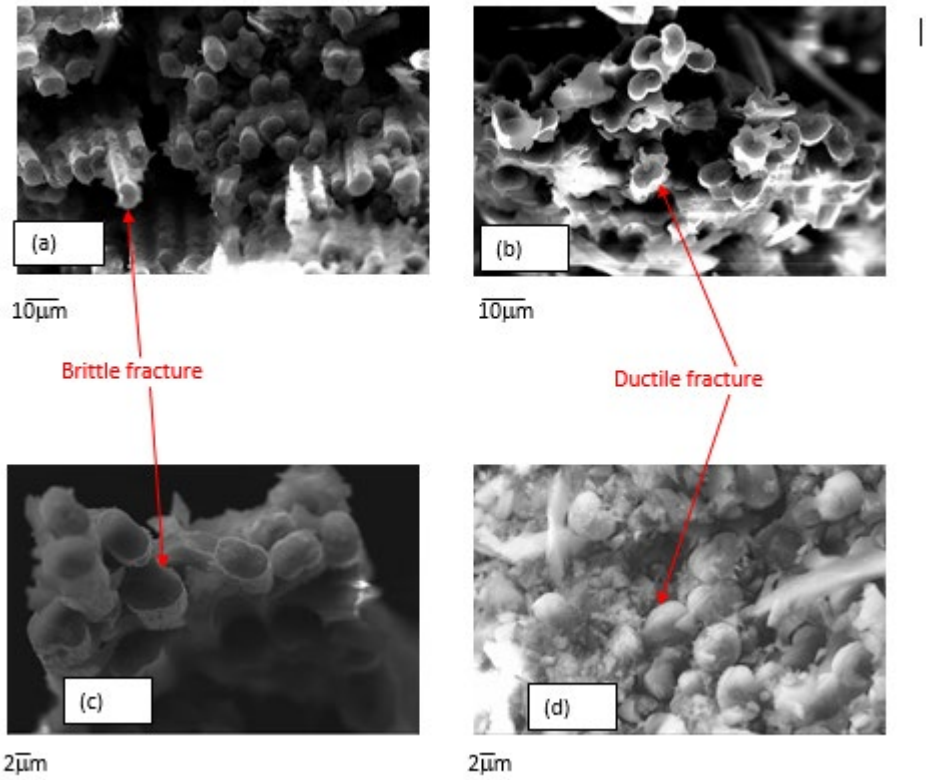

Fig. 37: Fracture surface of carbon fibres after impact test at (a, c)-40°C (b, d) RT.

Impact energy for room temperature impact tested sample is found to be slightly lower for the both mode of testing than that of the sample impact tested at -40°C. This may be due the fact that carbon fibre broke in ductile manner (cup and cone fracture, Fig. 37 b,d) at room temperature while broke in brittle manner (Fig. 37 a,c) at -40°C. Lowering of test temperature to -40°C, however, has very little effect on the impact energy since this lowering of temperature does not significantly affect the mode of failure.

5. Conclusions

1. The fracture toughness and impact energy absorption by carbon-epoxy composite is mainly governed by the mode of failure.

2. For crack arrester mode:

During three point bend test, delamination /Mode II failure is predominantly observed for un-notched and smaller notched (<2mm) specimen. The medium notched (>2mm) specimens show mixed mode failure, higher notched (>3mm) specimens show predominantly carbon fibre breaking /mode I failure. Here, number of delaminated layers is higher for the specimen tested at higher cross head speed (500mm/min). During charpy impact test at a strain rate of 103/s, greater energy is absorbed by these specimens by numerous delamination.

3. For crack divider mode: predominantly mode I failure occurs during three point bend test and impact test except for un-notched specimens which are failed by mixed mode.

4. It is observed in this study that impact energy absorption is highest in case of specimen failure by mode II, medium in case of mixed mode and lowest in case of Mode I failure. Therefore, during charpy test (strain rate 10^3/s) at crack arrester mode, the composite shows numerous delamination and absorbed much higher energy(~40J/cm^2) than that at crack divider mode (~10J/cm^2) where mode I failure is predominant.

5. It can be concluded from the above observation that presence any defect/discontinuity such as porosity/crack in the crack divider orientation is much more harmful than those present in crack arrester orientation. Since, even the presence of smallest crack/discontinuity at crack divider orientation favours mode I failure of the composite.

6. Lowering of test temperature to -40°C has very little effect on the impact energy since it does not significantly affect the mode of failure.

7. K1c and flexural strength of the composite is observed to be approximately 20MPa.m$^{0.5}$ and 640MPa respectively.

Author Contributions: conceptualization, K. M. Swarup, D. Jiten and S Seetaraman; methodology, K. M. Swarup, D. Jiten and S Seetaraman; validation, K. M. Swarup, D. Jiten and S Seetaraman; investigation, K. M. Swarup, D. Jiten and S Seetaraman; data curation, K. M. Swarup, D. Jiten and S Seetaraman; writing—original draft preparation, K. M. Swarup, D. Jiten and S Seetaraman; writing—review and editing, K. M. Swarup, D. Jiten; visualization, K. M. Swarup, D. Jiten. Authorship must be limited to those who have contributed substantially to the work reported.

Funding: DRDO has provided funding for this work.

Acknowledgments: The Authors wish to thank Dr. Partha Ghosal, Scientist-G and ADITYA RANJAN, TECHNICAL OFFICER 'A' for SEM study. They also would like to thank D S K Murali, Tapan Mallik and E Durga Rao for carrying out three point bend test and impact test respectively. They also wish to thank Dr. Archana Paradkar, Scientist-G, for giving permission to carry out impact test.They also wish to thank all the staffs of DMRL, DRDL and ASL for their help in experimental investigation. The authors also gratefully acknowledge DRDO for funding this work.

Conflicts of Interest: The authors declare no conflict of interest.

References

1. Sharma, S.P.; Lakkad, S.C. Impact behavior and fractographic study of carbon nanotubes grafted carbon fiber-reinforced epoxy matrix multi-scale hybrid composites. *Composites Part A* **2015**, *69*, 124–131.
2. Yu, Z.; Li, R.; Peng, Z.; Tang, Y. Carbon Fiber Reinforced Epoxy Resin Matrix. *Composites Materials Science: Advanced Composite Materials* **2017**, 1–6.
3. Baptista, R.; Mendão, A.; Guedes, M.; Marat-Mendes, R. An experimental study on mechanical properties of epoxy-matrix composites containing graphite filler. *Procedia Structural Integrity*, **2016**, *1*, 074–081.
4. Nie, H.J.; Xu, Z.; Tang, B.L.; Dang, C.Y.; Yang, Y.R.; Zeng, X.L.; i Lin, B.C.; Shen, X.J. The effect of grapheme oxide modified short carbon fibe on the interlaminal shear strength of cabon fiber fabric /epoxy composites. *Journal of MaterialsScience*, **2021**, *56*, 488-496.
5. Davis, D.C.; Wilkersona, J.W.; Zhu, J.; Ayewaha, D.O.O. Improvements in mechanical properties of a carbon fiber epoxy composite using nanotube science and technology. *Comosite structures*, **2010**, *92*, 2653–2662.
6. Paiva, J.M.F.; Santos, A.N.D.; Rezende, M.C. Mirabel Cerqueira Rezendec Mechanical and Morphological Characterizations of Carbon Fiber Fabric Reinforced Epoxy Composites Used in Aeronautical Field. *Materials Research*, **2009**, *12*, 367–374.
7. Bouette, B.; Cazeneuve, C.; Oytana, C.; Effect of strain rate on interlaminar shear properties of carbon/epoxy composites. *Composites Science and Technology*, **1992**, *45*, 313–321.
8. Khan, T.A.; Kim, H.; Kim, H.J. Fatigue delamination of carbonfiber-reinforced Polymer-matrix composites. in Failure Analysis in BioComposites, Fiber-Reinforced Composites and Hybrid Composites. Woodhead Publishing Series in Composites Science and Engineering, Edited by Jawaid, M.; Thariq, M.; Saba, N. 2019, 1-28. https://doi.org/10.1016/B978-0-08-102293-1.00001-2.
9. Li, X.; Yan, Y.; Guo, L.; Xu, C. Effect of strain rate on the mechanical properties of carbon/epoxy composites under quasi-static and dynamic loadings. *Polymer Testing*, **2016**, *52*, 254–264.
10. Brannigan, E. Carbon Composite Strengthening: Effects of Strain Rate Sensitivity and Feature Size, A Master Thesis of Science, Mechanical Engineering, in Texas Tech University, May, 2012.
11. Groves, S. E., Sanchez, R. J., Lyon, R. E. and Brown, A. E., High strain rate effects for composite materials. In *Composite Materials: Testing and Design*, Vol. 11, ASTM STP 1206, ed. E. T. Camponeschi. American Society for Testing and Materials, Philadelphia, 1993, pp. 162–176.
12. Daniel, I. M.; Hsiao, H. M.; Cordes, R. D. High Strain Rate Effects on Polymer, Metal and Ceramic Matrix Composites and Other Advanced Materials: (Aerospace Division AD - Proceedings) Hardcover – 1 January 1995, 48, pp. 167–177.
13. Melin, L. G.; Asp, L. E. Effects of strain rate on transverse tension properties of a carbon/epoxy composite: Studied by Moiré photography. *Composites A*, **1999**, *30*, 305–316.
14. Lenda, T.A.; Mridha, S. Impact Strength of Carbon Reinforced Epoxy Composite at Different Temperatures. *Advanced Materials Research*, **2011**, *264-265*, 451-456.
15. Smiley, A. J.; Pipes, R. B. Rate Effects on Mode I Interlaminar Fracture Toughness in Composite Materials. *Journal of Composite Materials*, **1987**, *21*, 670–687.
16. Maikuma, H.; Gillespie, J. W.; Wilkins, D. J. Mode II Interlaminar Fracture of the Center Notch Flexural Specimen under Impact Loading. *Journal of Composite Materials*, **1990**, *24*, 124-149.
17. Chapman, T. J.; Smiley, A. J.; Pipes, R. B. Proc. ICCMG/ECCM2, F. L. Matthews, N. C. R. Buskell, J. M. Hodgkinson, and J. Morton, eds. New York, 1987; p 3.295.
18. Kusaka, T.; Yamauchi, Y.; Kurokawa, T. Effects of strain rate on mode II interlaminar fracture toughness in carbon-fibre/epoxy laminated composites. *Journal De Physique IV*, **1994**, *4*, C8–671-676.
19. Kusaka, T.; Kurokawa, T.; Hojo, M.; Ochiai, S. Dynamic Effects in Hopkinson Bar Four-Point Bend Fracture. *Key Engineering Materials*, **1998**, *141–143*, 477–498.
20. Kageyama, K.; Kimpara, I. Delamination failures in polymer composites. *Materials Science and Engineering A*, **1991**, *143*, 167–174.

21. Bisht, A.; Dasgupta, K.; Lahiri, D. Investigating the role of 3D network of carbon nanofillers in improving the mechanical properties of carbon fiber epoxy laminated composite. *Composites Part A*, **2019**, *126*, 105601.
22. Toygar, M.E.; Toparli, M.; Uyulgan, B. An investigation of Fracture Toughness of Carbon/Epoxy Composites. *Journal of Reinforced Plastics and Composites*, **2006**, *25*, 1887–1895.
23. Quan, D.; Urdaniz, J.L.; Ivankovic, A. Enhancing mode-I and mode-II fracture toughness of epoxy and carbon fibre reinforced composites using multi-walled carbon nanotubes. *Materials and Design*, **2018**, *143*, 81-92.
24. Turla, P.; Kumar, S.S.; Reddy, P.H.; Shekar, K.C. Processing and Flexural Strength of Carbon Fiber and Glass Fiber Reinforced Epoxy-Matrix Hybrid Composite, *International Journal of Engineering Research & Technology (IJERT)* **2014**, *3* (4), April.
25. Srivastava, A.K.; Gupta, V.; Yerramalli, C.S.; Singh, A. Flexural strength enhancement in carbon-fiber epoxy composites through graphene nano-platelets coating on fibers. *Composites Part B*, **2019**, *179*, 107539.
26. Shingare, K.; Shendokar, S.M.; Deshmukh, P.V.; Chavan, S.S. Analysis of Flexural Properties of Carbon Fiber Reinforced / E-Poxy Composite Material. *International Engineering Research Journal*, **2015**, *3*, 495-498.
27. Md, E.I.; Tanjheel, H.M.; Mahesh, V.H.; Shaik, J. Characterization of Carbon Fiber Reinforced Epoxy Composites Modified with Nanoclay and Carbon Nanotubes. *Procedia Engineering* **2015,** *105,* 821 – 828.